

CNRS
Centre National de la Recherche Scientifique

INFN
Istituto Nazionale di Fisica Nucleare



– VSR4 calibration –
Stability from June 2010 to September 2011
(VSR3 and VSR4)

L. Rolland

VIR-0703A-11

November 24, 2011

VIRGO * A joint CNRS-INFN Project
Project office: Traversa H di via Macerata - I-56021 S. Stefano a Macerata, Cascina (PI)
Secretariat: Telephone (39) 50 752 521 – Fax (39) 50 752 550 – e-mail virgo@pisa.infn.it

Contents

1	Introduction	2
2	Dark fringe timing and sensing	2
2.1	<i>Pr_B1_ACp</i> and <i>Pr_B1p</i> channels	2
2.2	Shaping filters on <i>Pr_B1_d{2,3}_ACp</i>	3
3	Calibration of the mirror actuation	5
3.1	Mirror actuation in HP mode	5
3.2	Mirror actuation in LN1 mode	5
3.2.1	Stability of the LN1/HP ratio measurements	7
3.2.2	Comparison of VSR3 parameterizations with latest data	11
3.3	Mirror actuation in LN2 mode	13
3.3.1	Stability of the LN2/HP ratio measurements	13
3.3.2	Comparison of pre-VSR4 parameterizations with latest data	16
4	Calibration of the WE and NE marionette actuations	18
4.1	1st period: time stability up to July 26th 2011	18
4.2	2nd period: new parameterizations from July 26th 2011	18
5	Conclusions	22
A	Appendix: Mirror actuation	25
A.1	Mirror actuation in HP mode: stability (June 2010 to Sept. 2011)	25
A.2	LN1/HP measurements	29
A.2.1	LN1/HP stability (June 2010 to Sept. 2011)	29
A.2.2	Comparison of VSR3 parameterization with latest data	43
A.3	LN2/HP ratio	47
A.3.1	LN2/HP stability (May to September 2011)	47
A.3.2	Comparison of the pre-VSR4 parameterization with VSR4 data	56
B	Appendix: Marionette actuation	58
B.1	Marionette actuation: evolution (June 2010 to Sept. 2011)	58

1 Introduction

This note gives the status of the Virgo calibration during the Virgo 4th Science Run (VSR4, June 3rd to September 5th, 2011). Calibration data were taken the week before the run. Since the actuation was not changed since VSR3, the stability of the calibration data are studied over more than one year, starting in June 2010¹.

The methods are the same as described in [1], [2] and [3]. The preliminary VSR4 calibration was released in [6].

The modifications of the interferometer (ITF) between VSR3 and VSR4 are not expected to modify the calibration (timing and actuation). A modification in the dark fringe sensing is expected to be transparent for calibration:

- use of shaping filter (nominally 2 Hz – 12 Hz, 2nd order) in the readout of the dark fringe photodiodes, channels *Pr_B1_d2,3_ACp*. The reverse shaping filters have been implemented in *Pr*.

However, modifications were done during VSR4 with impact on the actuation:

1. Up to July 5th 2011², the mirror actuation was used in the so-called *Low-Noise 1* (LN1) mode. The end mirror actuation has then been switched to *Low-Noise 2* (LN2) mode since actuation DAC noise appears to limit the sensitivity. However, the end mirror actuation had been calibrated both in LN1 and LN2 modes before VSR4 [6].
2. The marionette actuation (NE and WE) was modified on July 26th 2011³: new resistors added to decrease the DAC noise and update of the filters in the DSP. The modification was preliminary tested for calibration on July 19th 2011⁴.

2 Dark fringe timing and sensing

A synoptic of the general sensing of the dark fringe channels is shown in the figure 1 of [2].

2.1 *Pr_B1_ACp* and *Pr_B1p* channels

It was shown in [6] that **the timing and sensing of the dark fringe channels did not change since VSR2 and VSR3. The models given in the table 1, p.3 of [5] are still valid for VSR4.**

¹ Stored in files with calibration period 961000000_999000000.

²See logbook entry 29832

³See logbook entry 29971

⁴See logbook entry 29932

2.2 Shaping filters on $Pr_B1_d\{2,3\}_ACp$

Up to May 2011, the readout of the dark fringe channels $Pr_B1_d\{2,3\}_ACp$ did not use any shaping filter. In the same ADC board, channels with shaping filters⁵ have been used from end of May 2011. The reverse shaping filters have been setup in the Pr configuration such that the sum of the two signals, Pr_B1_ACp , does not depend on the channel that is used (flat or shaped).

Preliminary shaping filters measurements had been done at LAPP few years ago. Direct measurements could be done in the data since two channels are stored for each photodiode:

- $Pr_B1_d\{2,3\}_ACp_flat$ without shaping filter, at 20 kHz (as before),
- $Pr_B1_d\{2,3\}_ACp_shap$ with shaping filter, at 20 kHz, and before the reverse shaping is applied in Pr .

The TF $Pr_B1_d\{2,3\}_ACp_shap/Pr_B1_d\{2,3\}_ACp_flat$ is thus a measurement of the shaping filter (the digital Butterworth filter being the same for both channels). It is precisely measured with the ITF locked in step 12, during wide band noise injections, in particular during the Virgo TF measurements. Measurements from May 31st⁶ have been used to fit the shaping filters and update the Pr configuration before VSR4⁷.

A monitoring of the shaping filters stability have been done using the weekly measurements of the Virgo TF. The shaping filter TF from June 3rd 2011 is used as reference⁸. It is then compared to the TF measured every week. The comparison with the TF measured on September 5th 2011⁹ is shown figure 1. The shaping filters look stable during VSR4.

The compensation of the shaping filter is processed in the Pr process such that the sensing TF is not modified when switching the controls from $Pr_B1_d\{2,3\}_ACp_flat$ to $Pr_B1_d\{2,3\}_ACp_shap$. The compensation is defined by the filters measured on June ??? 2011. The stability of the shaping filters indicates that **the switches that occurred during VSR4 are indeed transparent for the calibration point of view.**

⁵Nominally second order filters, with zero at 2 Hz, pole at 12 Hz, Q s of 0.5

⁶GPS 990890828, 5 minutes.

⁷See logbook entries 29510 and 29518

⁸From GPS 991143310 to 991143610

⁹From GPS 999238190 to 999238490

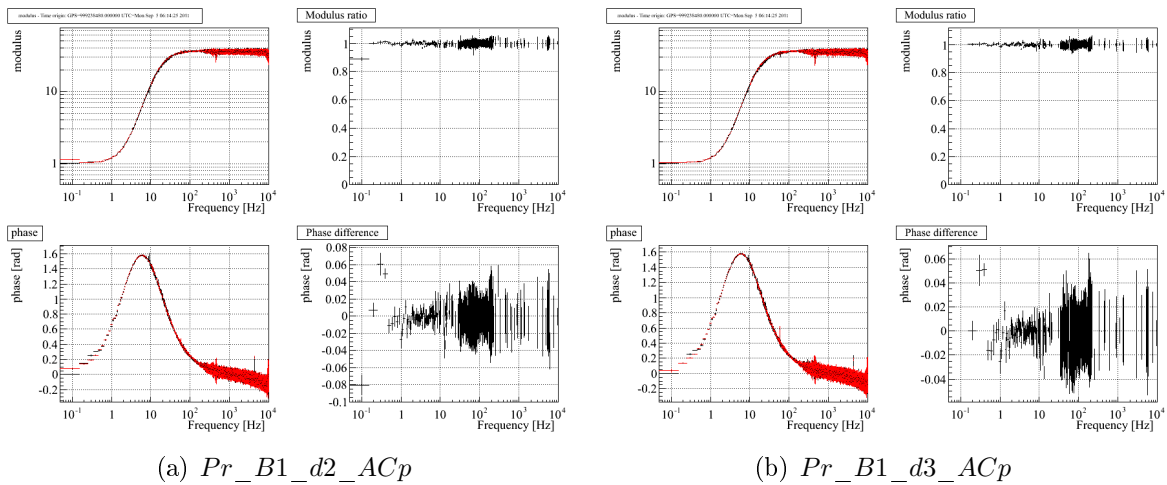


Figure 1: Comparison of the shaping filter used on B1 in June 3rd and September 5th 2011. For each photodiode, two columns are shown: Left: modulus and phase of the TFs (red: black:); Right: modulus ratio and phase difference. Only the data with coherence higher than 99% are shown.

3 Calibration of the mirror actuation

The mirror actuation is defined as the TF (with modulus in m/V) from the correction signal to the induced mirror motion. The time reference is the GPS time.

In the plots that are shown, the actuation is corrected for the mechanical model of the pendulum, defined as a 2nd order low-pass filters with $f_0 = 0.6$ Hz and $Q = 1000$.

In this section, we describe:

1. the stability of the mirror actuation in HP mode over VSR3 and VSR4,
2. the stability of the LN1/HP mirror actuation ratio over VSR3 and VSR4, with the hint for temperature dependence at high frequency,
3. the stability of the LN2/HP end mirror actuation ratio over VSR4.

3.1 Mirror actuation in HP mode

As usual, the mirror actuation in HP mode is extracted from data in free swinging Michelson, with excitation of the mirrors at different frequencies with sine signals.

No change is expected in the mirror actuation in HP mode from VSR3 to VSR4. The VSR3 and VSR4 measurements have thus been compared. Examples of time evolution are given for the WE mirror actuation in HP mode, using the U-D coils, in figure 2. Similar figures for other mirror actuation are given in appendix A.1.

End mirrors – For most of the measurements of the end mirror actuation, the hypothesis of a stable transfer function over the year is in agreement with the statistical errors. This is always the case for the phase which is measured within few mrad. Some larger variations are sometimes observed in modulus, but they do not exceed 1% (see figure 11).

BS mirror – For the BS mirror actuation, the statistical errors are much lower and systematic errors arise in modulus. In particular, a trend for a 2% decrease of the modulus between VSR3 and VSR4 is observed (see figure 14). Concerning the phase, no variation is observed within few mrad.

3.2 Mirror actuation in LN1 mode

Since no change is expected in the mirror actuation in LN1 mode between VSR3 and VSR4, the VSR4 measurements have been compared to the VSR3 measurements. In this section, we show that time variations are observed but are still within the systematic errors estimated on the LN1 mirror actuation parameterizations. As a consequence, in LN1 mode, the actuation

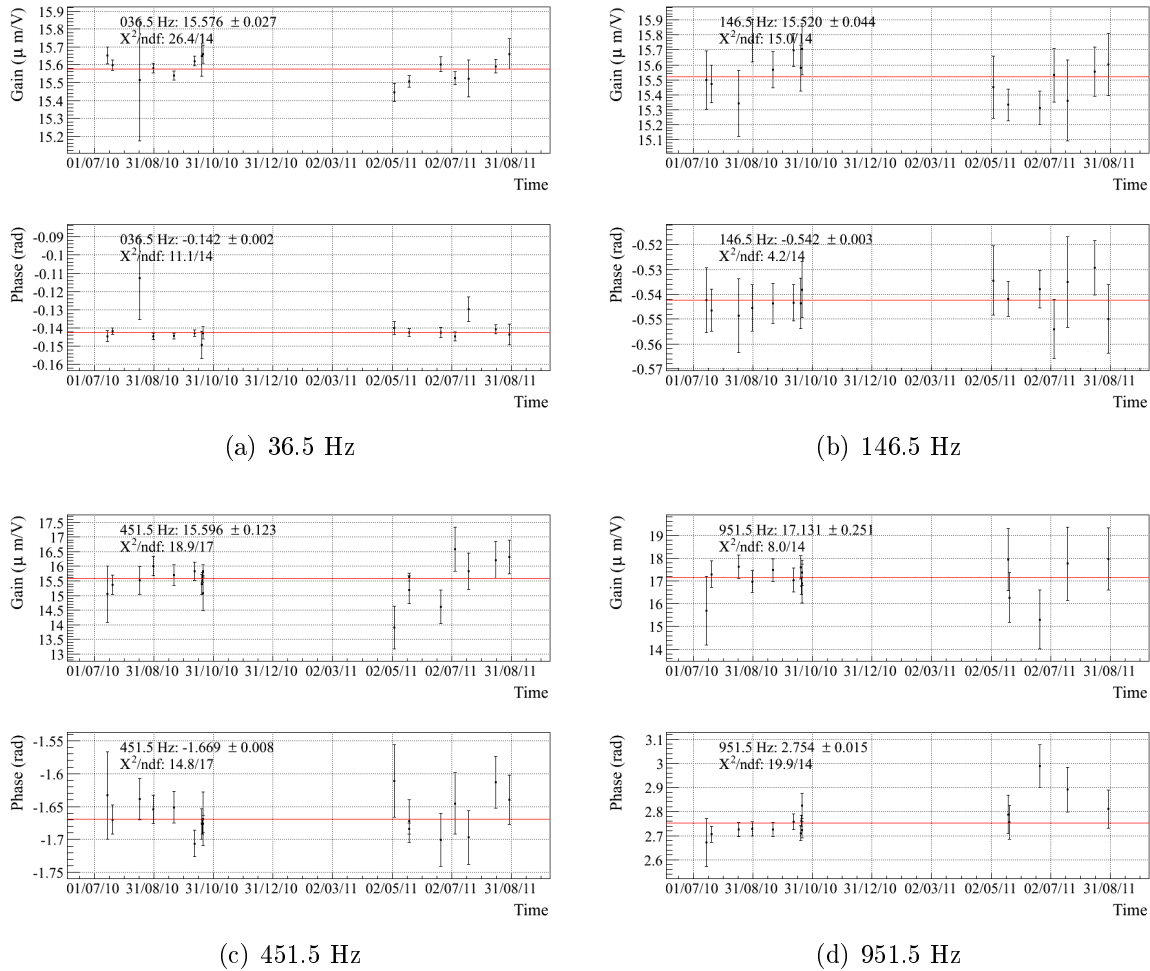


Figure 2: Evolution as function of time (June 2010 to September 2011) of the measured mirror actuation in HP mode for the up-down coils of the WE mirror at four different frequencies.

parameterizations computed for VSR3 [5] can be used for VSR4.

As usual, the mirror actuation in LN1 mode is done (for the 12 coils) in two measurement steps:

- measurement of the mirror actuation in HP mode, extracted from data in free swinging Michelson,
- measurement of the LN1/HP ratio of the actuation, extracted from the actuation current response,
- extraction of the mirror actuation in LN1 mode from the two former results.

3.2.1 Stability of the LN1/HP ratio measurements

As during VSR3, during the run weekly measurements, the LN/HP measurements were done using mainly white noise injections. On the contrary, pre-VSR4 measurements had been performed through line injections mainly. Note that the amplitude of the signal at a given frequency is larger when injecting this particular frequency than wide band noise (inducing smaller statistical errors), but the total amplitude (peak-to-peak) of the signal is larger when injecting wide band noise.

With respect to VSR3 datasets, the lines around 8 Hz were not injected and the white noise low frequency range increased from 4 Hz to 10 Hz (in order not to excite the 8 Hz θ_z oscillation of the end mirror payloads).

The figure 3 shows the time evolution of LN1/HP measurements at some frequencies for the up coil of WE, from July 2010 to September 2011. The figure 4 shows the same measurements but given as function of the amplitude (peak-to-peak) of the current flowing in the coil. Similar figures for all the coils of WE, NE and BS can be found in appendix A.2.

Different comments can be made regarding these measurements (and are summarized for each coil in table 1):

1. as during VSR3, some non-linearities arise for some coils: the modulus ratio is different by a few percent depending on the amplitude of the injected noise (the difference arise mainly between lines and white noise injections).
2. as during VSR3, the phase difference (LN-HP) decreases when the amplitude of the injected noise increases (except for NE coils). This variations looks like an additionnal delay of $\sim 3 \mu\text{s}$ ($\sim 20 \text{ mrad}$ at 1036 Hz).
3. for some (6) coils, the modulus ratio changed by a few percent between VSR3 and VSR4.

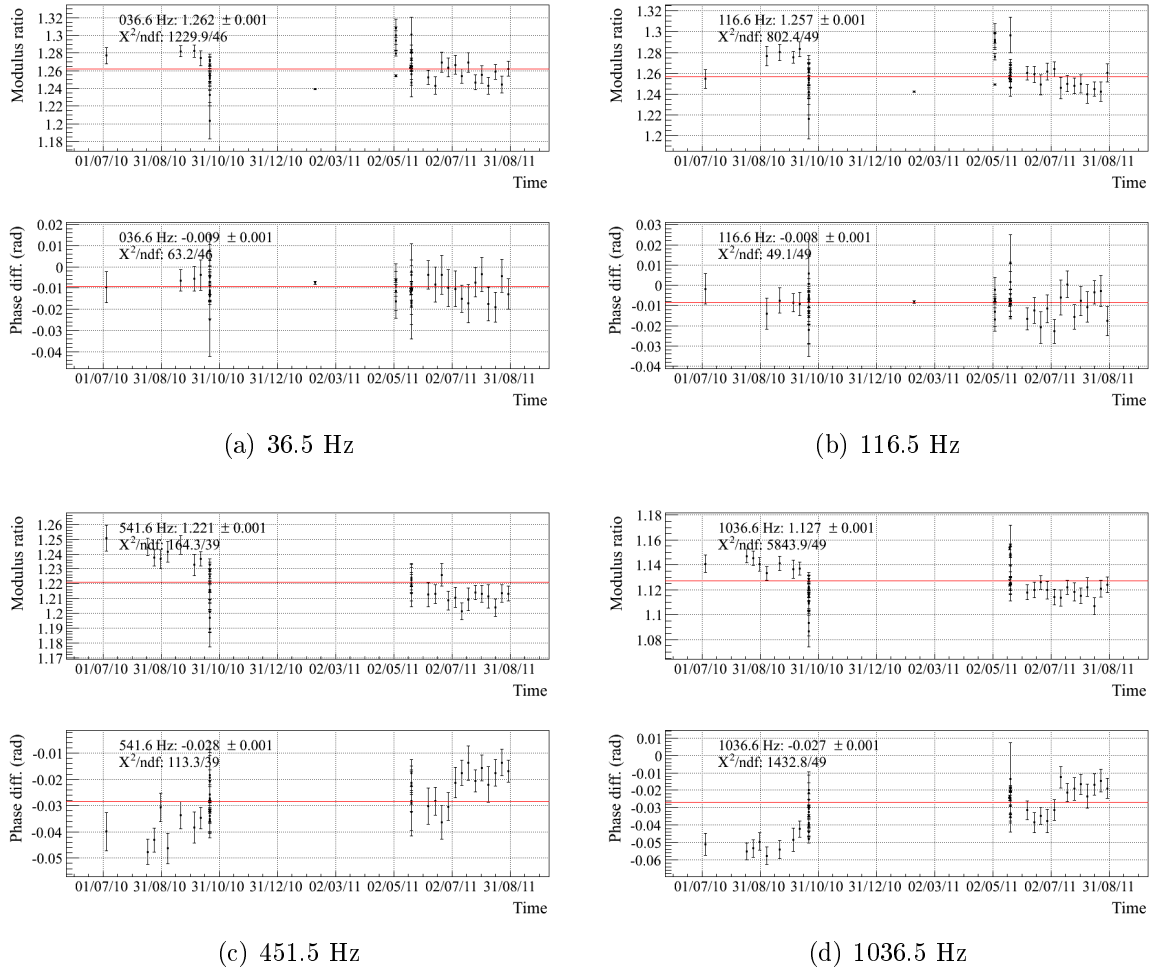


Figure 3: Evolution as function of time (June 2010 to May 2011) of the measured actuation TF ratio (LN1/HP) for the up coil of the WE mirror at four different frequencies.

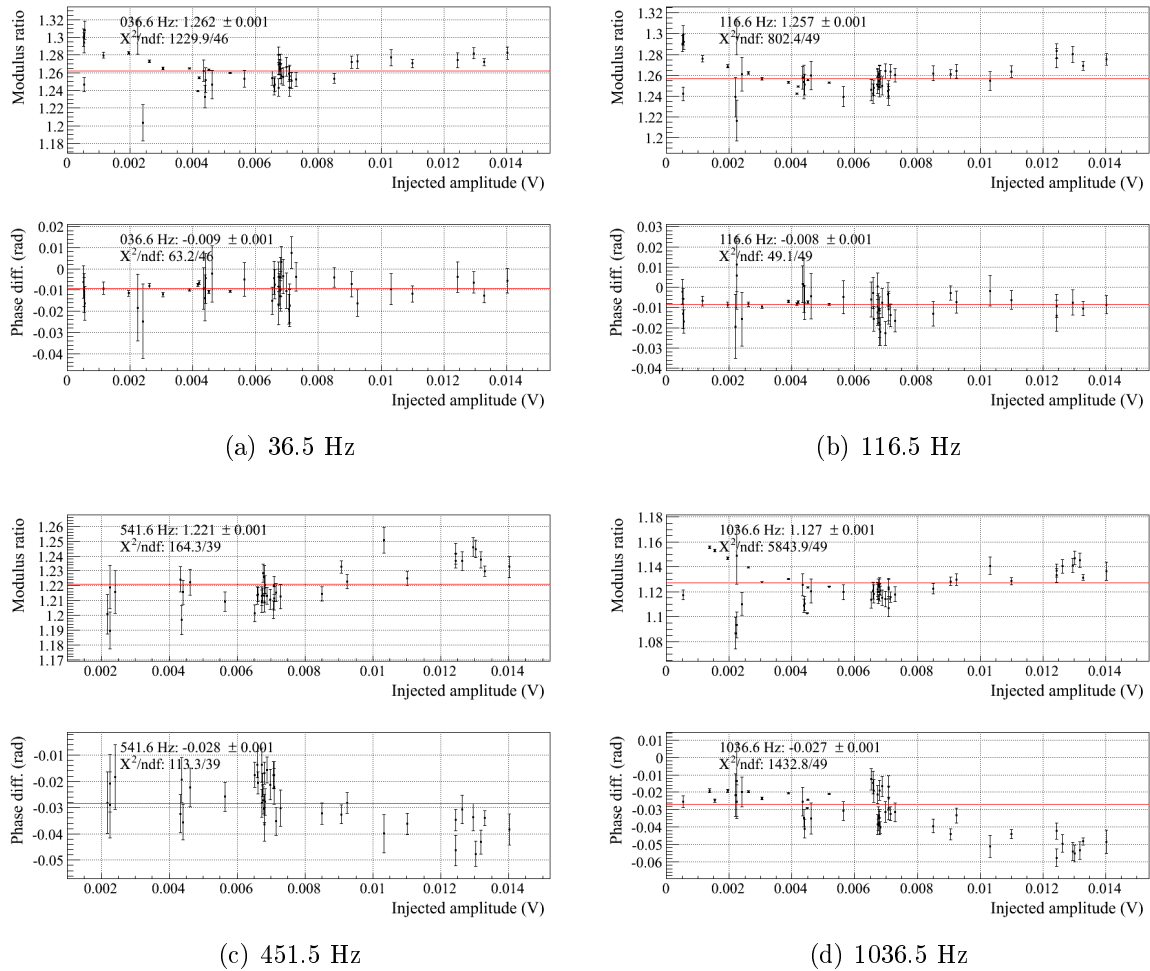


Figure 4: Evolution as function of the signal amplitude of the measured actuation TF ratio ($LN1/HP$) for the up coil of the WE mirror at four different frequencies. The amplitude in the x-axis is the amplitude of $V1 : Ca_WE_RM_CoilU$ during the injections in LowNoise mode.

4. for the Up and Down coils of NE and WE, the measured phase difference increased when the mirror actuation was switched to LN2 for data taking (July 5th 2011, after the calibration measurements). This increase looks like a reduction of the actuation delay by $\sim 1.5 \mu\text{s}$ ($\sim 10 \text{ mrad}$ at 1036 Hz). Note that it happens only on the four coils switched to LN2 mode and used in the longitudinal control loop.

Coil	Non-linearities		VSR3 \rightarrow VSR4	LN1 \rightarrow LN2 (July 5th 2011)
	modulus	timing		
WE-U	-	+3 μs	-2%	-1.5 μs
WE-D	-	+3 μs	-2%	-1.5 μs
WE-L	-1%	-	-2%	-
WE-R	+3%	+3 μs	-	-
NE-U	-	-	-	-1.5 μs
NE-D	< 1%	-	-	-1.5 μs
NE-L	-	-	-	-
NE-R	-2%	-	+1%	-
BS-UL	+8%	+3 μs	-	-
BS-UR	-	+3 μs	+3%	-
BS-DL	< 1%	+3 μs	+1%	-
BS-DR	-	+3 μs	+2%	-

Table 1: Details for each coil of the variations commented in the text (LN1 mode). The non-linearities confirm the VSR3 behaviour. The variations between VSR3 and VSR4 are new systematic errors. The variations after the switch to LN2 mode are not included in the final systematic errors.

Comments (2) and (4) can be explained by an increase of the delay introduced by the actuation when the electronics temperature increases: for (2), the temperature might increase when increasing the injected noise, and the actuation delay increases ; for (4), when using the LN2 mode in standard condition, the average temperature of the LN1 electronics might have decreased, and the actuation delay decreases. With this interpretation, the effect could be due to a temperature change at the level of the DAC, the coil driver or the coil itself. This is reasonable as it would represent, for example, a variation of 1% of the nominal delay introduced by the DAC anti-image filter of 190 μs . However, the NE up and down coils are sensitive to effect (4) but not to (2).

Both effects are compatible with the **systematic error of 3 μs set on the mirror actuation phase in LN1 mode** in previous notes.

As explained in previous calibration notes, the effect (1) is reduced since an average of the LN1/HP ratio is performed per each coil, and then over the coils used in the actuation. It reduces the effect of the coil non-linearities by a factor 2 for the end mirror and a factor 4 for the BS mirror. A systematic error of 3% had been set on the modulus.

Concerning the variations between VSR3 and VSR4 (effect 3), the variations are of the same order as the systematic errors on the modulus estimated during VSR3 (3%) and might increase the final estimation for VSR4. For the BS mirror, the HP actuation modulus was found to have decreased by 2%, which is compensated by the LN1/HP increase of $\sim +2\%$.

As a conclusion, a **systematic error of 4% on the mirror actuation modulus in LN1 mode** seems reasonable.

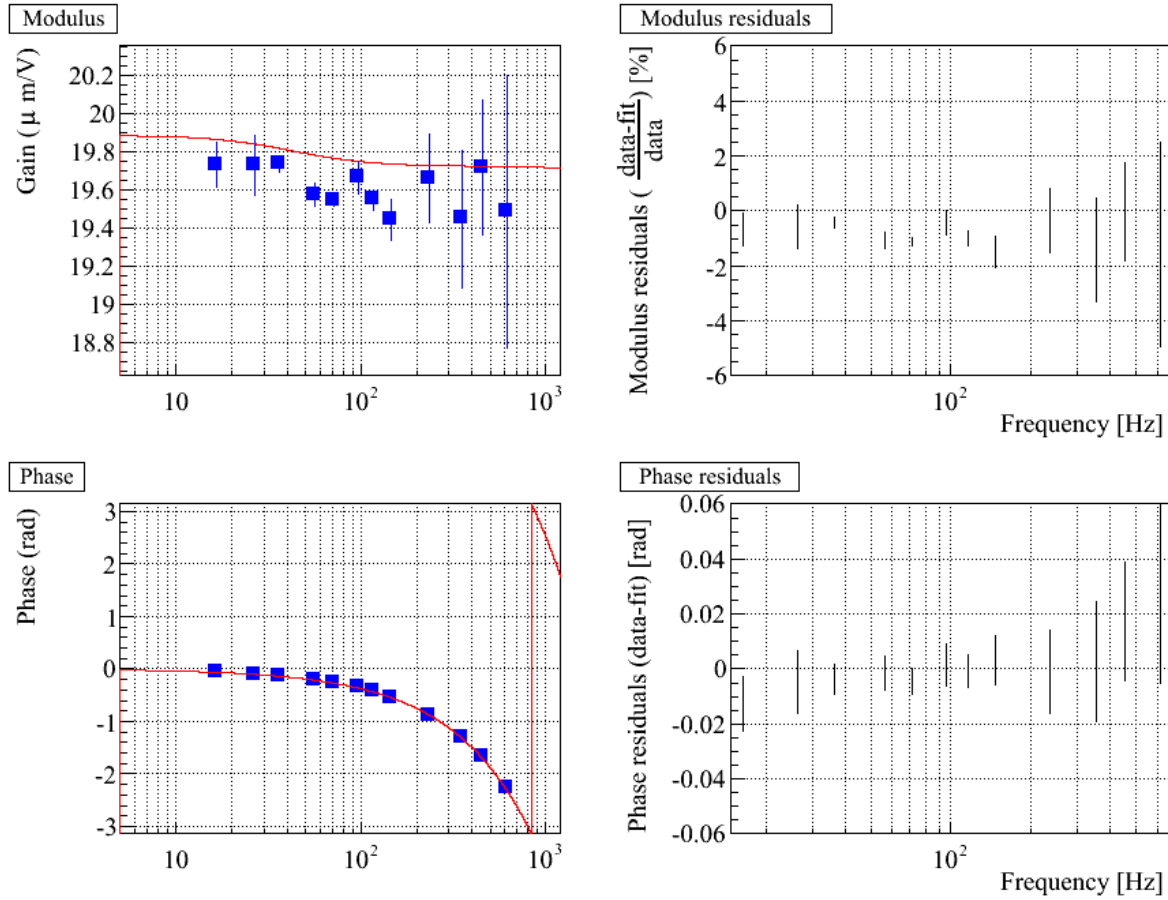
3.2.2 Comparison of VSR3 parameterizations with latest data

In figure 5 and figures in appendix A.2.2, the VSR4 measurements are compared with the actuation parameterizations derived from VSR3 data and used for online processes during VSR4 (the one described in tables 3 and 4, p. 10,11 of note [5]). The HP actuation has been derived using all the VSR4 data (June to September 2011). The LN1/HP actuation ratio has been derived: (i) using all the VSR4 data for the BS, NE,L-R and WE,L-R actuations, and (2) using data from June to July 5th 2011 for the NE,U-D and WE,U-D actuations (in order to be independent of the slight phase variations observed between VSR3 and VSR4 and when switching to LN2 mode).

The comparison highlights that the parameterized modulus is larger slightly ($\sim 1\%$) larger than the data for the end mirrors, while the parameterized phase is compatible with the data. The BS actuation parameterization is still in agreement with the data.

Such differences are within the systematic errors estimated above and must be related to the fact that the LN1/HP ratio measurement was not done in exactly the same conditions as for VSR3 (number of line injections vs number of white noise injections). However, in order to be conservative, **a systematic error of 1% can be added on the LN1 mirror actuation** from this comparison.

Larger difference are observed for NE,L-R actuation, but these coils were not used during VSR4 (no blind injections).



(a) WE, U-D

Figure 5: *WE, U-D mirror actuation in LN1 mode. Left: comparison of VSR3 model (red) with VSR4 averaged measurements (blue). Right: residuals.*

3.3 Mirror actuation in LN2 mode

The mirror actuation in LN2 mode is done in two measurement steps, as for the LN1 measurement:

- measurement of the mirror actuation in HP mode, extracted from data in free swinging Michelson,
- measurement of the LN2/HP ratio of the actuation, extracted from the actuation current response,
- extraction of the mirror actuation in LN1 mode from the two former results.

3.3.1 Stability of the LN2/HP ratio measurements

The figures 6 and 7 show the LN2/HP ratio up coil of WE mirror as function of time during preVSR4 and VSR4 (May to September 2011), and as function of the amplitude (peak-to-peak) of the current flowing in the coil. Similar figures for all the coils of the end mirrors are given in appendix A.3.

The statistical errors of the measurements are about a factor 3 to 4 larger than for the LN1/HP measurements. This is expected since the maximum injected noise in LN2 channel is limited by a factor 4 compared to the LN1 channel.

The LN2/HP ratio measurements (in similar conditions every Tuesday) are stable during VSR4 withing statistical errors.

When including the pre-VSR4 measurements when the amplitude of the injections was varied (injecting mainly lines instead of wide-band noise), some systematic errors arise, possibly related to non-linearities or time variations of less than 2% in the actuation for the following coils:

- WE, D: visible at low frequency only,
- WE, R: the gain varies by 4% between pre-VSR4 and VSR4 data,
- NE, D: time variations ?
- NE, R: the gain varies by 5% between pre-VSR4 and VSR4 data (coil not used during VSR4).

No significant change of the measurement appears on July 5th 2011 from when the data in Science Mode were taken in LN2 mode (except for the right coil of NE, whose gain increased by 8% and delay reduced by 9 μ s, but this coil was not used during VSR4 and this issue in meaningless for calibration point of view).

The left coil of NE has a gain which is about half the nominal one. But again, this coil was not used during VSR4.

As a conclusion, **the systematic errors of the LN2/HP ratio measurements are similar to the ones of the LN1/HP measurements.**

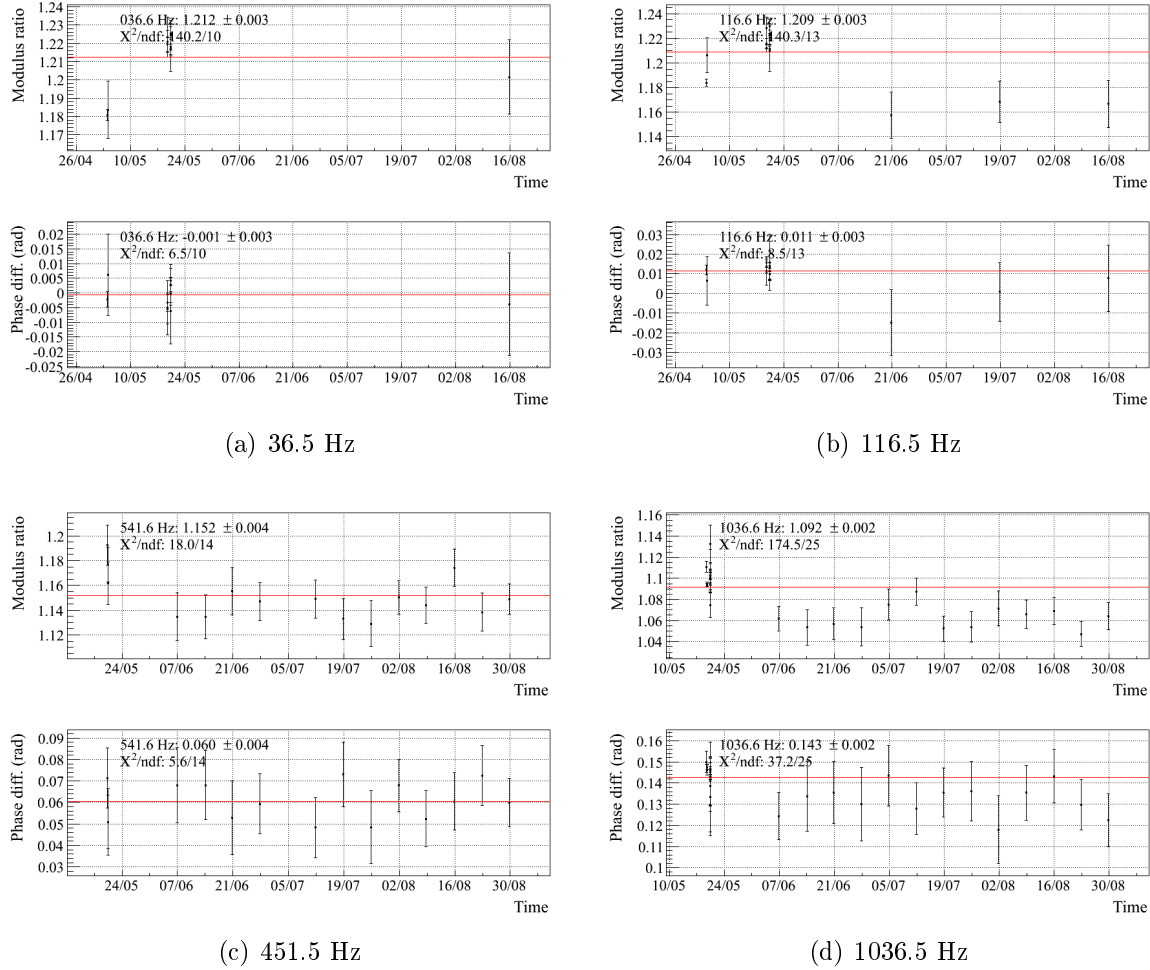


Figure 6: Evolution as function of time (June 2010 to May 2011) of the measured actuation TF ratio (LN2/HP) for the up coil of the WE mirror at four different frequencies.

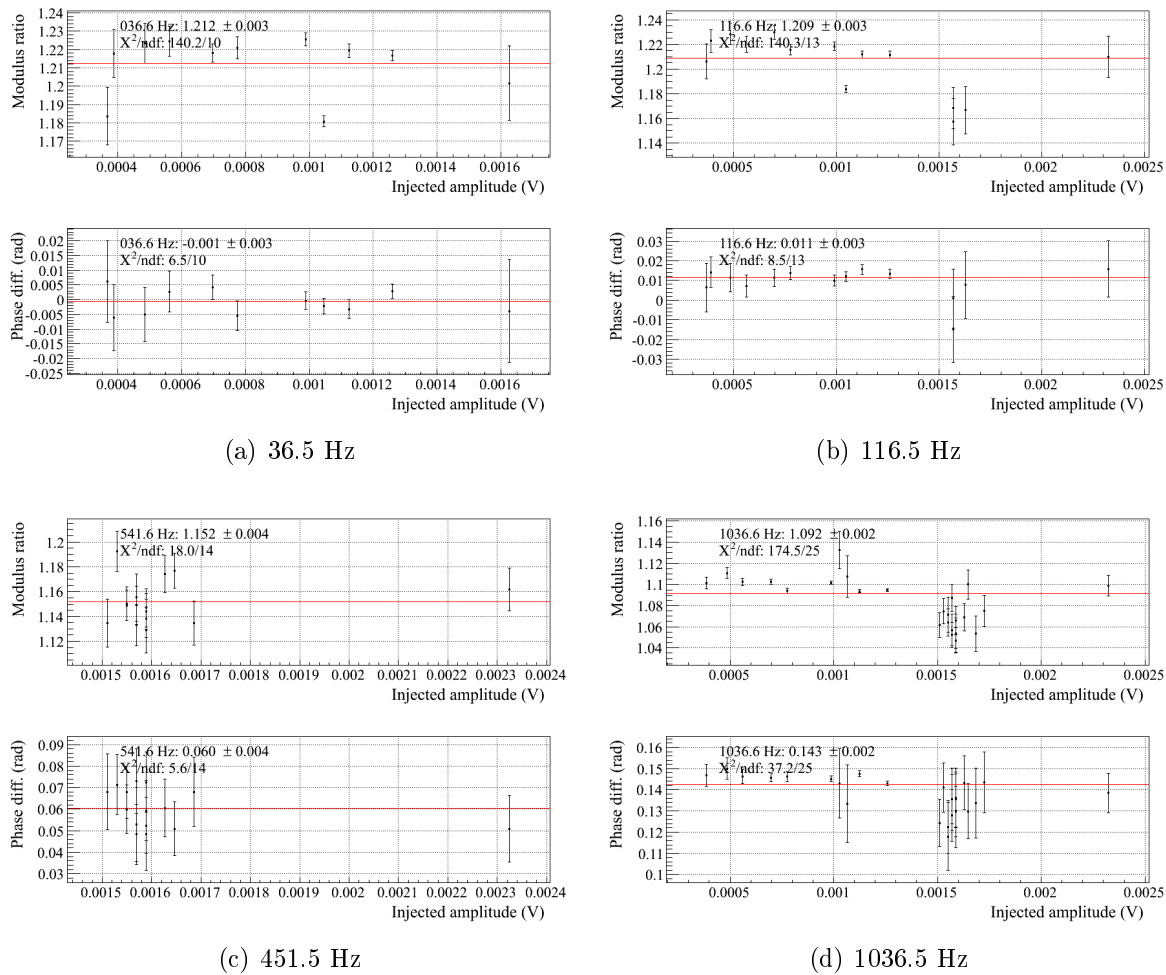


Figure 7: Evolution as function of the signal amplitude of the measured actuation TF ratio ($LN2/HP$) for the up coil of the WE mirror at four different frequencies. The amplitude in the x -axis is the amplitude of $V1 : Ca_WE_RM_CoilU$ during the injections in LowNoise mode.

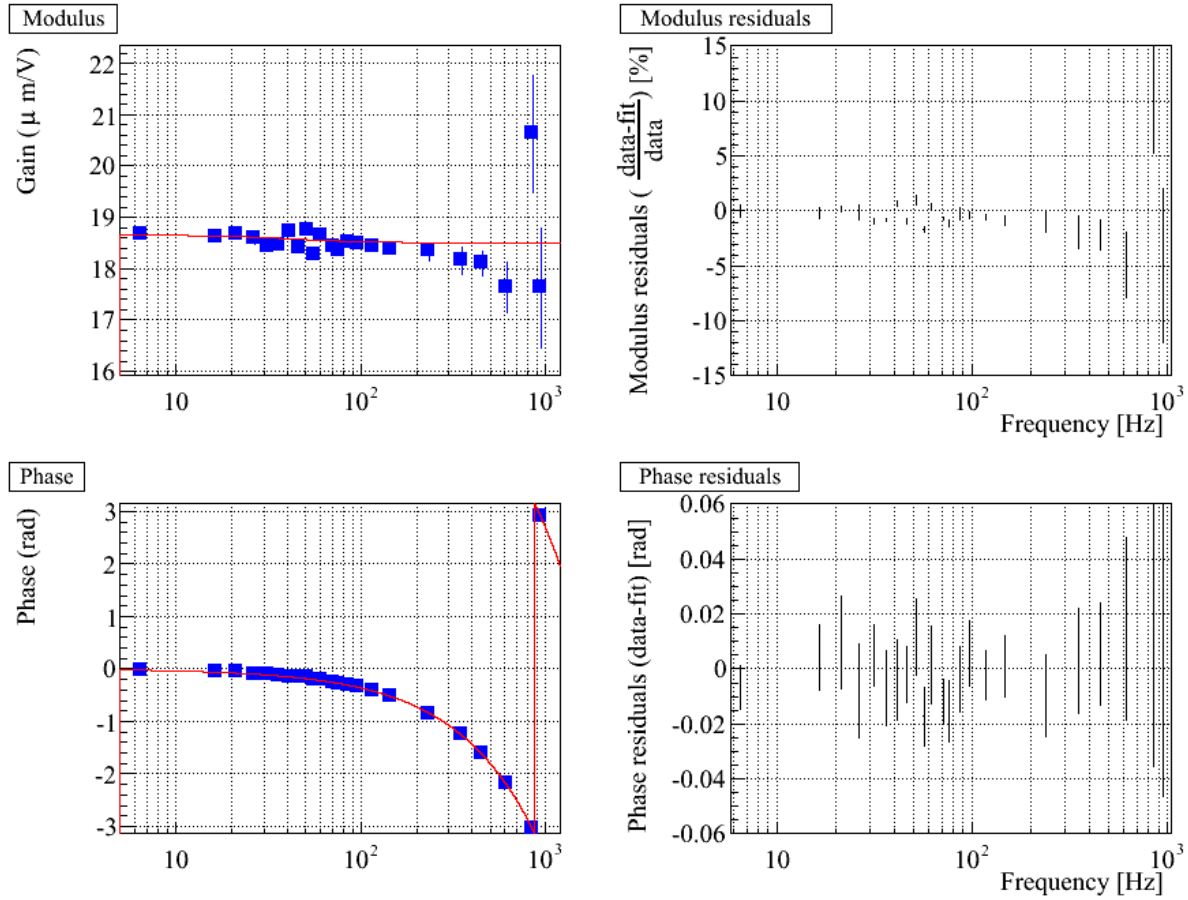
3.3.2 Comparison of pre-VSR4 parameterizations with latest data

The comparison of the VSR4 measurements with the LN2 actuation parameterizations derived using the pre-VSR4 data (and used in the online processes during the run) is shown in figure 8 for WE, using U-D coils, and in appendix A.3.2 for the other actuations.

The three actuations parameterizations (WE,U-D, WE,L-R and NE,U-D) are consistent with the phase parameterizations. Concerning the modulus, some difference, up to $\sim 2\%$ are seen:

- WE,U-D: agreement within 2% up to 1 kHz,
- WE,L-R: agreement within 2% up to 700 Hz, with a trend to larger discrepancy at larger frequencies,
- NE,U-D: agreement within 2% up to 1 kHz.

As a conclusion, the parameterizations of the end mirror actuation in LN2 mode, derived before VSR4 and given in table 1, p.14, of note [6], are valid. From this comparison, **a systematic error of 2% can be added on the LN2 mirror actuation.**



(a) WE, U-D

Figure 8: *WE, U-D mirror actuation in LN2 mode. Left: comparison of pre-VSR4 model (red) with all VSR4 averaged measurements (blue). Right: residuals.*

4 Calibration of the WE and NE marionette actuations

The marionette actuation is defined as the TF (with modulus in m/V) from the correction signal to the induced mirror motion¹⁰ (i.e. Sc_{WE, NE_zM}). The time reference is the GPS time.

In the plots that are shown, the actuation is corrected for the mechanical model of the pendulum, defined as **two** 2nd order low-pass filters with $f_0 = 0.6$ Hz and $Q = 1000$.

Two studies are performed:

1. the data up to July 26th 2011 are compared to VSR3 data to check for marionette actuation stability,
2. a new parameterization is extracted from the data from July 26th 2011 and compared to the one set online during VSR4.

4.1 1st period: time stability up to July 26th 2011

The figures in **B** show the time evolution of the WE and NE marionette to mirror actuation ratio (in LN1 mode), at some frequencies, from July 2010 to September 2011. Thanks to a better sensitivity at low frequency, the measurement during VSR4 are better than the one from VSR3.

No significant variation is observed up to July 26th 2011, where a sudden change is seen on both modulus and phase, related to the change of hardware.

As a conclusion, for the data up to July 26th 2011, the VSR3 parameterizations given in table 6, p.50 of note [5] are still valid, with the same systematic errors: **3% in modulus and 30 mrad in phase up to 150 Hz**.

4.2 2nd period: new parameterizations from July 26th 2011

The parameterizations of the marionette actuations used online from July 26th 2011 during VSR4 is given in table 2. They had been estimated from few (2?) sets of measurements done on July 19th 2011.

The data from July 19th 2011¹¹ to the end of VSR4 have been used to derive the NE and WE marionette actuations. The measurements are compared to the initial parameterization in figures 9 and 10.

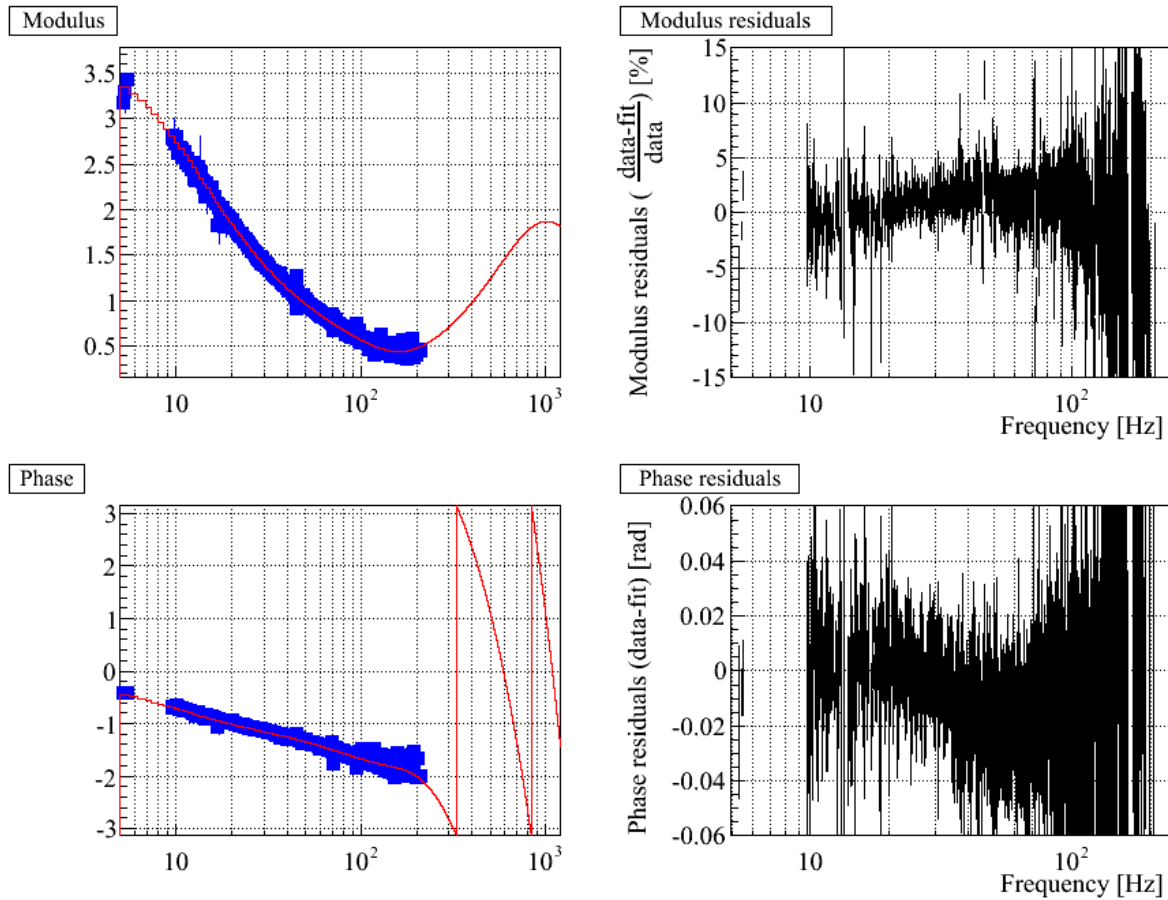
¹⁰ The marionette longitudinal actuation is done through two coils (left and right). Emphasis filters are set in the DSP for both coil channels in order to compensate for de-emphasis filters used in the coil drivers. At the beginning of VSR4, the resistance of the coil channel was $R \sim 16.5 \Omega$ and its inductance $L \sim 214$ mH: the L-R circuit resulted in a pole $R/(2\pi L)$ around 12 – 13 Hz. From July 26th 2011, the resistance has been increased.

¹¹A preliminary change of marionette had been done on July 19th (logbook 29932) in order to measure the marionette actuation and prepare the parameterization to be ready when the change would be permanent, which was decided on July 26th.

The residuals between all the data and the parameterization can be used as an estimate of the systematic errors: **5% in modulus and 50 mrad in phase, up to 150 Hz.**

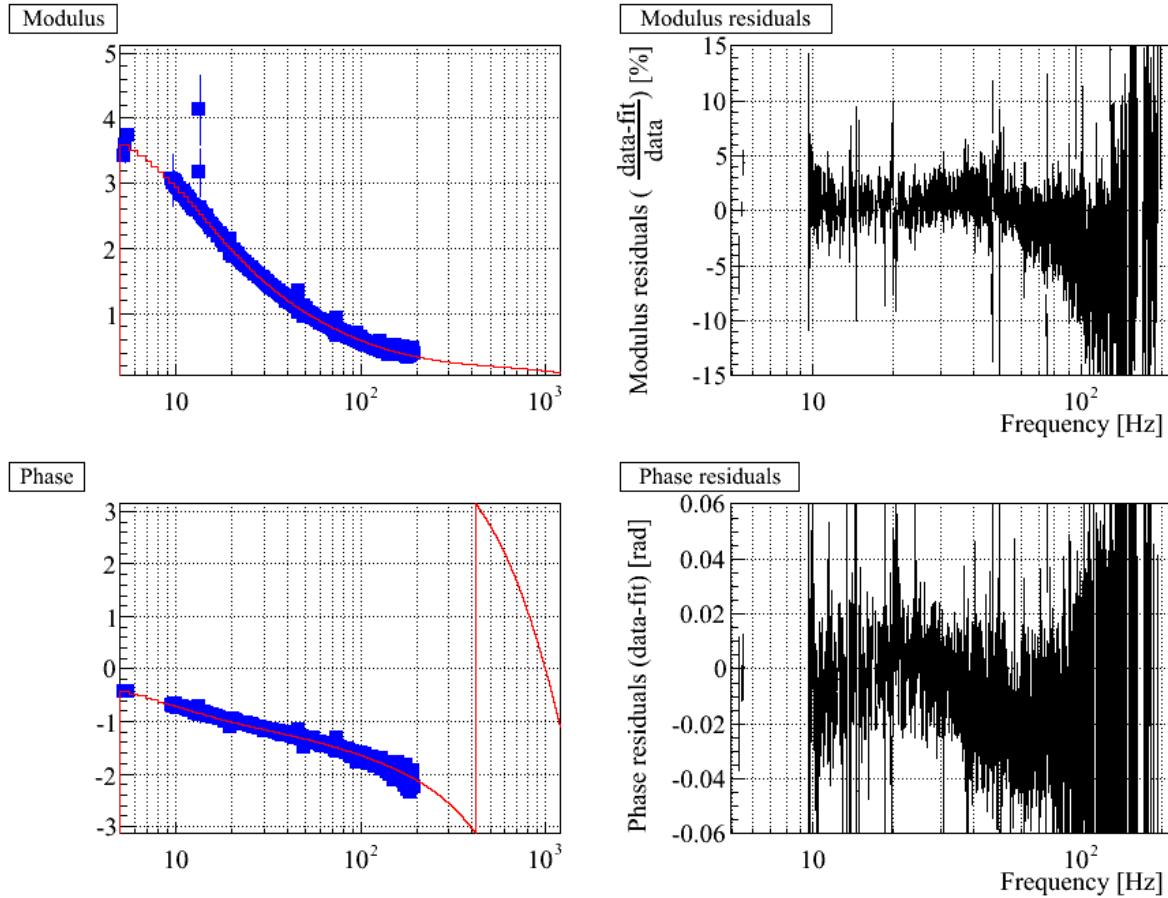
	WE	NE
Gain ($\mu\text{m}/\text{V}$)	3.729 ± 0.022	3.988 ± 0.023
Raw delay (μs)	$(1809) \pm 21$	(701.2 ± 21)
Delay (μs)	1659.7 ± 21	551.9 ± 21
Φ_0 (rad)	0	0
Pole frequency (Hz)	85.1 ± 5.3	54.9 ± 2.1
Zero frequency (Hz)	43.8 ± 1.5	374.0 ± 28
Pole frequency (Hz)	10.51 ± 0.13	10.55 ± 0.11
Zero frequency (Hz)	–	37.73 ± 1.4
Complex zero f_0 (Hz)	167.6 ± 1.28	–
Complex zero Q	0.935 ± 0.025	–
2nd order low-pass Pendulum	$f_0 = 1000 \text{ Hz}, Q = 0.7$ Two 2nd order low-pass filters: $f_0 = 0.6 \text{ Hz}, Q = 1000$	
χ^2/ndf	2223.2/2503	1968.3/2450

Table 2: **WE and NE marionette actuation parameterizations** as estimated from data of July 19th 2011. Fit computed from 5 Hz to 200 Hz. The χ^2/ndf of the fits are given. Residuals are within better than 5% in modulus and 50 mrad in phase up to 150 Hz. The raw delays are the delay measured using the raw delays from the mirror actuation measurements. The delay has been corrected for the PrCa and sensing delays to take as reference the correction channels (i.e. Sc_WE_zMar): $\text{delay} = \text{raw_delay} - 100 - 49.3 \mu\text{s}$. Applying these TFs to the correction channels Sc_WE_zMar should enable to estimate the induce motion at absolute GPS time.



(a) WE, Marionette

Figure 9: *WE marionetta actuation, starting from July 26th 2011. Left: comparison of online model (red) with all data averaged after July 19th 2011 (blue). Right: residuals.*



(a) NE, Marionette

Figure 10: NE marionette actuation, starting from July 26th 2011. Left: comparison of online model (red) with all data averaged after July 19th 2011 (blue). Right: residuals.

5 Conclusions

Pre-VSR4 calibration measurements have been performed in May 2011 (4th and 20-22nd). It allowed to validate the stability of the calibration parameters since VSR3 (dark fringe sensing and timing, WE, NE and BS mirror actuation in LN1 mode and WE, NE marionette actuation). It also allowed to prepare the parameterizations for the end mirror actuation in LN2 mode. The results can be found in note [6].

During VSR4 (June to September 2011), the calibration parameters have been updated for the online processes following some changes in the ITF configuration. We can thus define **three periods**:

- June 3rd to July 5th 2011: same calibration parameters as during VSR3 [5],
- From July 5th: deal with the end mirror actuation in LN2 mode, with the parameterization given in [6],
- From July 26th: use the new marionette parameterization given in table 2.

A weekly monitoring of the calibration parameters has been done during VSR4. It confirmed that the **dark fringe sensing** calibration did not change during VSR4. Systematic errors on absolute timing are estimated to $\pm 4 \mu\text{s}$, from 1 Hz to 10 kHz.

Weekly measurements also allowed to check a posteriori that the **mirror actuation parameterizations (WE, NE and BS)** used online were good enough to describe the VSR4 data. We have shown in this note that:

- the parameterizations used online correctly describes the data,
- since some slight differences arise between the data and the parameterizations, the systematic errors are slightly larger than the ones estimated for VSR3. The errors are summarized in the following table.

		LN1 (Up to July 5th)		LN2 (From July 5th)	
		Modulus	Phase	Modulus	Phase
stat.	HP	1%	10 mrad	1%	10 mrad
	LN/HP	0.1%	1 mrad	0.3%	3 mrad
syst.	HP	–	–	–	–
	LN/HP	4%	3 μs	4%	3 μs
	Old param.	1%	–	2%	–
	Sensing timing	–	1 μs	–	1 μs
	Absolute timing	–	4 μs	–	4 μs
Total		5%	10 mrad/5 μs	5%	10 mrad/5 μs

The **PR mirror actuation** is not expected to have change between VSR3 and VSR4. It was not measured in 2011 and the same parameterization as the one for VSR3 [5] is thus used for VSR4.

The calibration of the **NE and WE marionette actuation** has two periods. The systematic errors are estimated from both the residuals between the parameterization and the data, and the errors on the mirror actuation in LN1 mode:

- Up to July 26th 2011: the model from VSR3 is valid up to 150 Hz, with systematic errors of 6% (3% and 5%) and 30 mrad in modulus and phase,
- From July 26th 2011: the model given in table 2 is valid up to 150 Hz, with systematic errors of 7% (5% and 5%) and 50 mrad in modulus and phase.

References

- [1] T. Accadia et al. (Virgo collaboration), *Class. Quantum Grav.* 28 (2011) 025005 *Calibration and sensitivity of the Virgo detector during its second science run* ([arXiv:1009.5190](#)).
- [2] L. Rolland *Calibration status in September 2009* (2009) [VIR-0576A-09](#).
- [3] L. Rolland *VSR2 mirror and marionette actuator calibration* (2010) [VIR-0076B-10](#).
- [4] L. Rolland, F. Marion, B. Mours, *Mirror and marionette actuation calibration for VSR1* (2008) [VIR-015B-08](#).
- [5] L. Rolland *Virgo calibration during VSR3* (2010) [VIR-0610A-10](#).
- [6] L. Rolland *Preliminary VSR4 calibration (June 2011)* (2011) [VIR-0336A-11](#).

A Appendix: Mirror actuation

A.1 Mirror actuation in HP mode: stability (June 2010 to Sept. 2011)

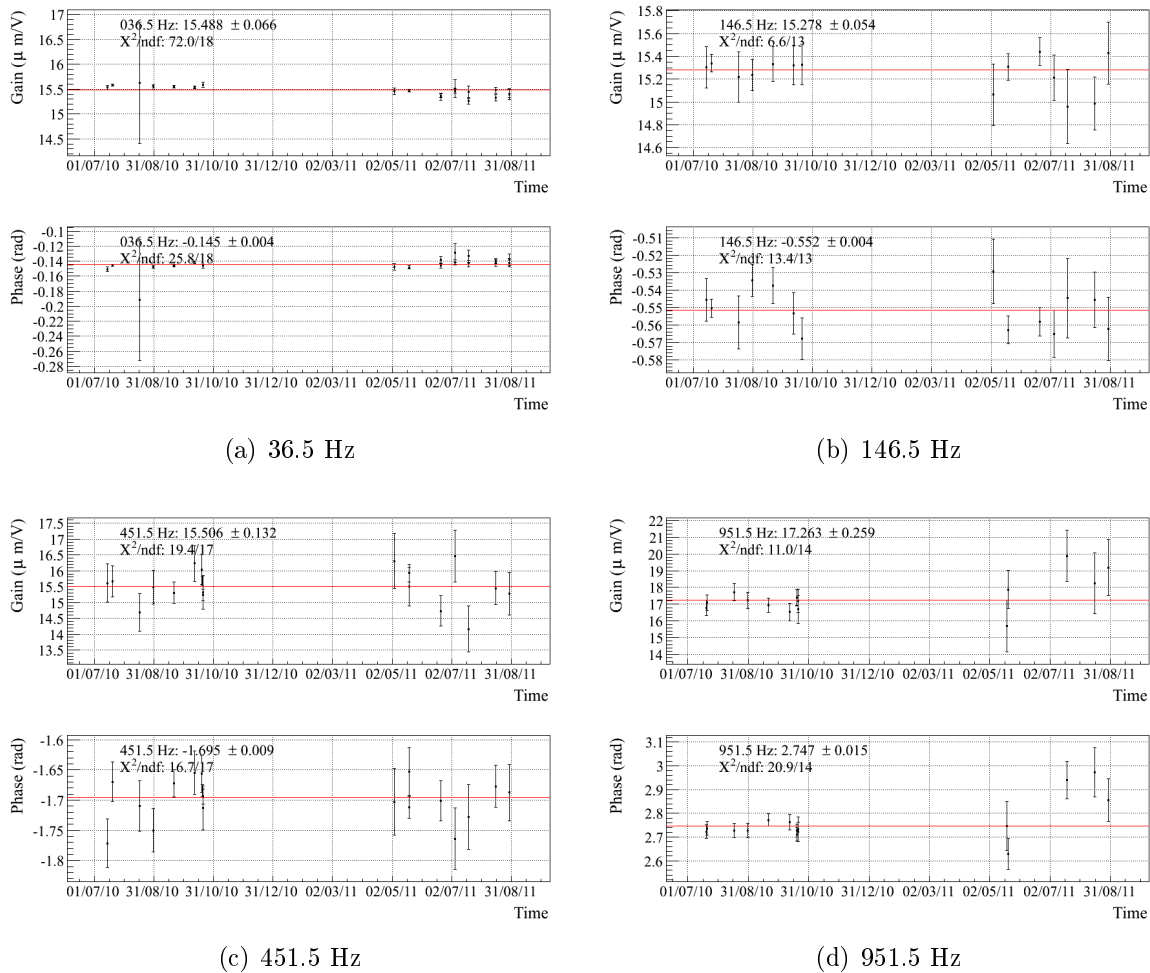


Figure 11: Evolution as function of time (June 2010 to September 2011) of the measured mirror actuation in HP mode for the left-right coils of the WE mirror at four different frequencies.

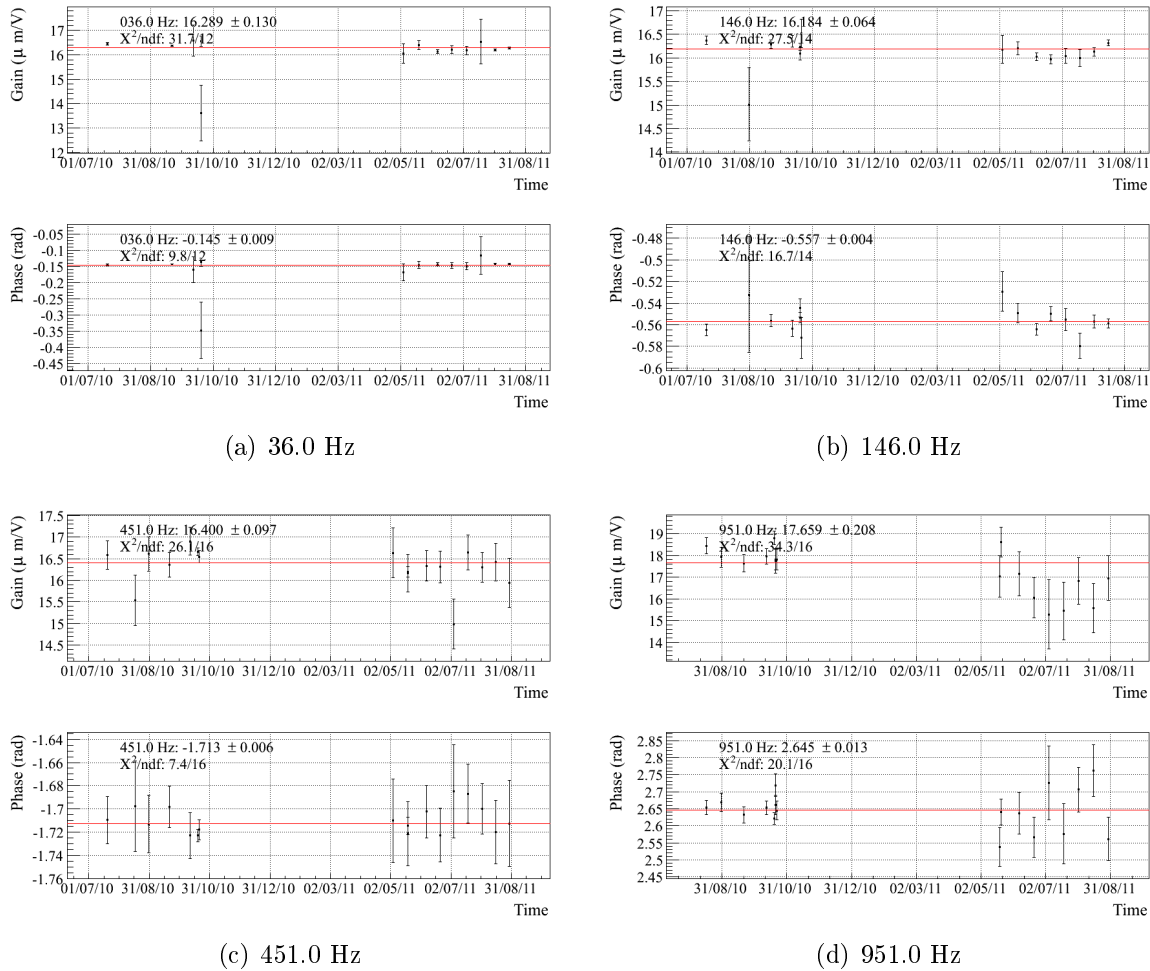


Figure 12: Evolution as function of time (June 2010 to September 2011) of the measured mirror actuation in HP mode for the up-down coils of the NE mirror at four different frequencies.

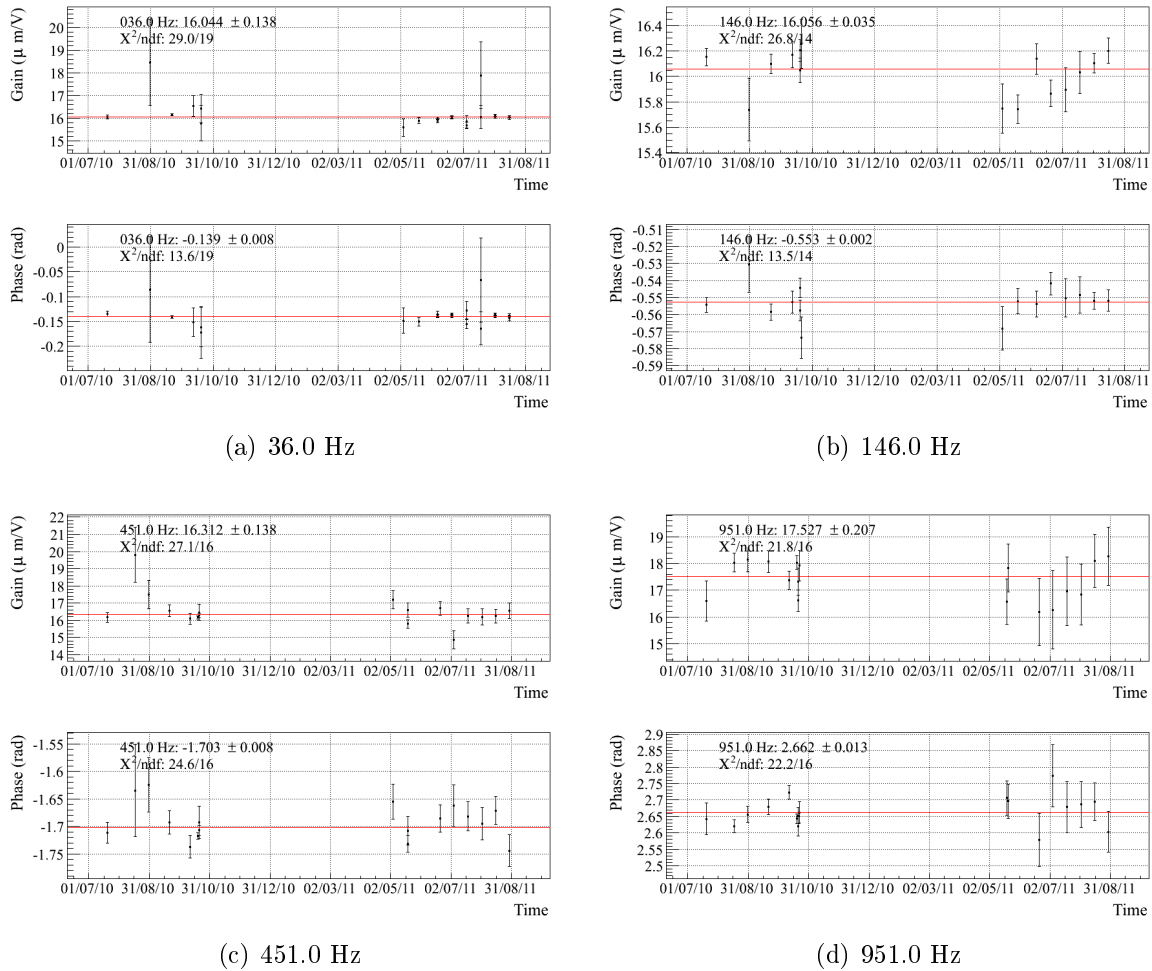


Figure 13: Evolution as function of time (June 2010 to September 2011) of the measured mirror actuation in HP mode for the left-right coils of the NE mirror at four different frequencies.

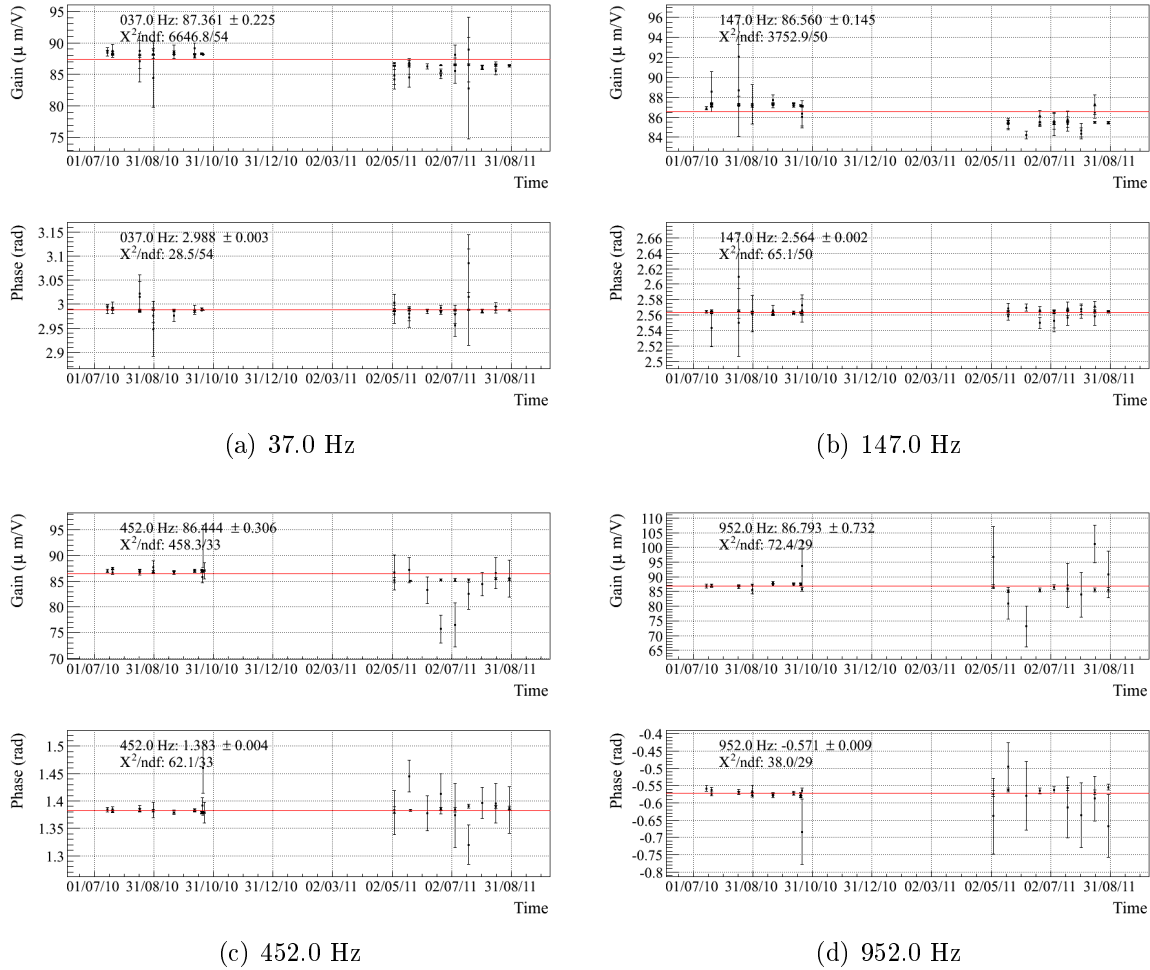


Figure 14: Evolution as function of time (June 2010 to September 2011) of the measured mirror actuation in HP mode of the BS mirror at four different frequencies.

A.2 LN1/HP measurements

A.2.1 LN1/HP stability (June 2010 to Sept. 2011)

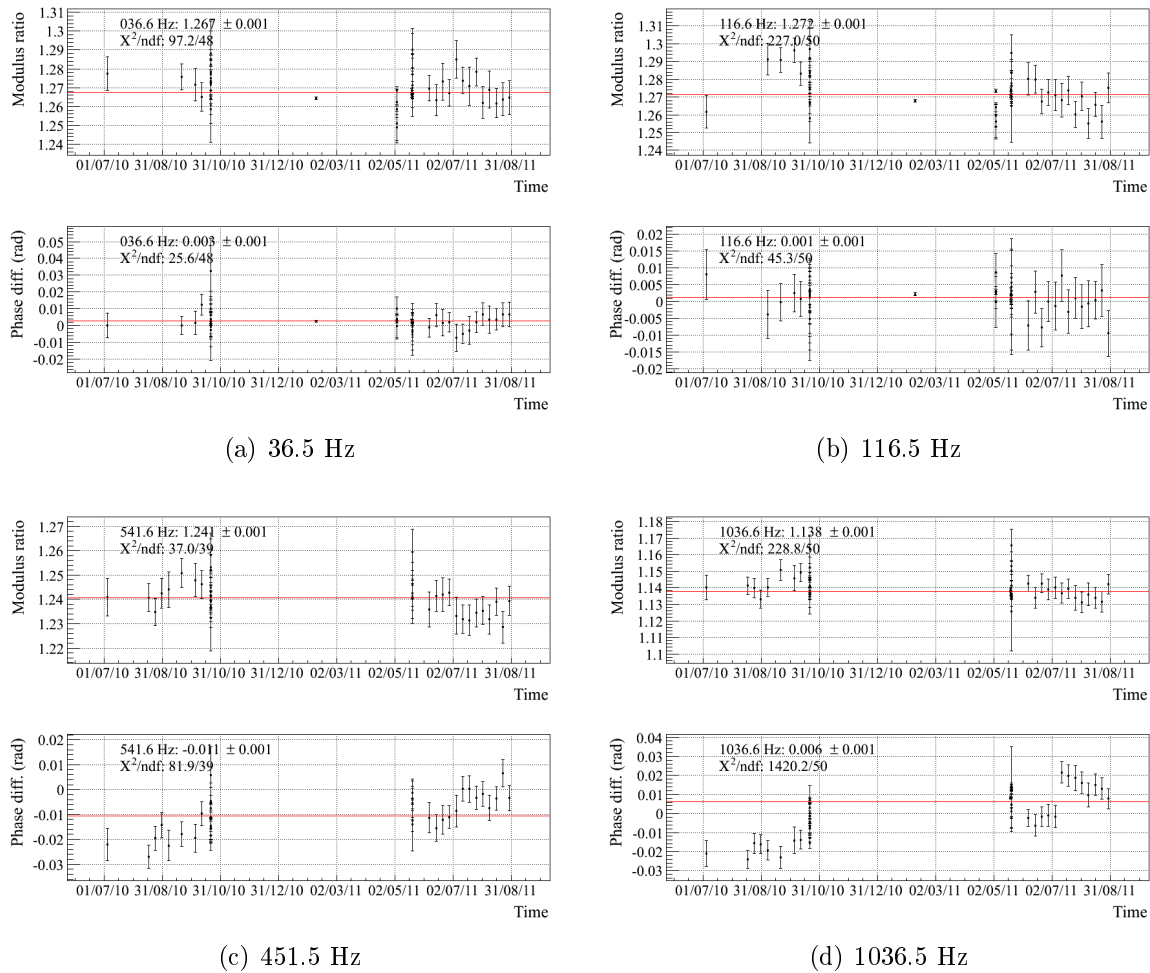


Figure 15: Evolution as function of time (June 2010 to September 2011) of the measured actuation TF ratio (LN1/HP) for the down coil of the WE mirror at four different frequencies.

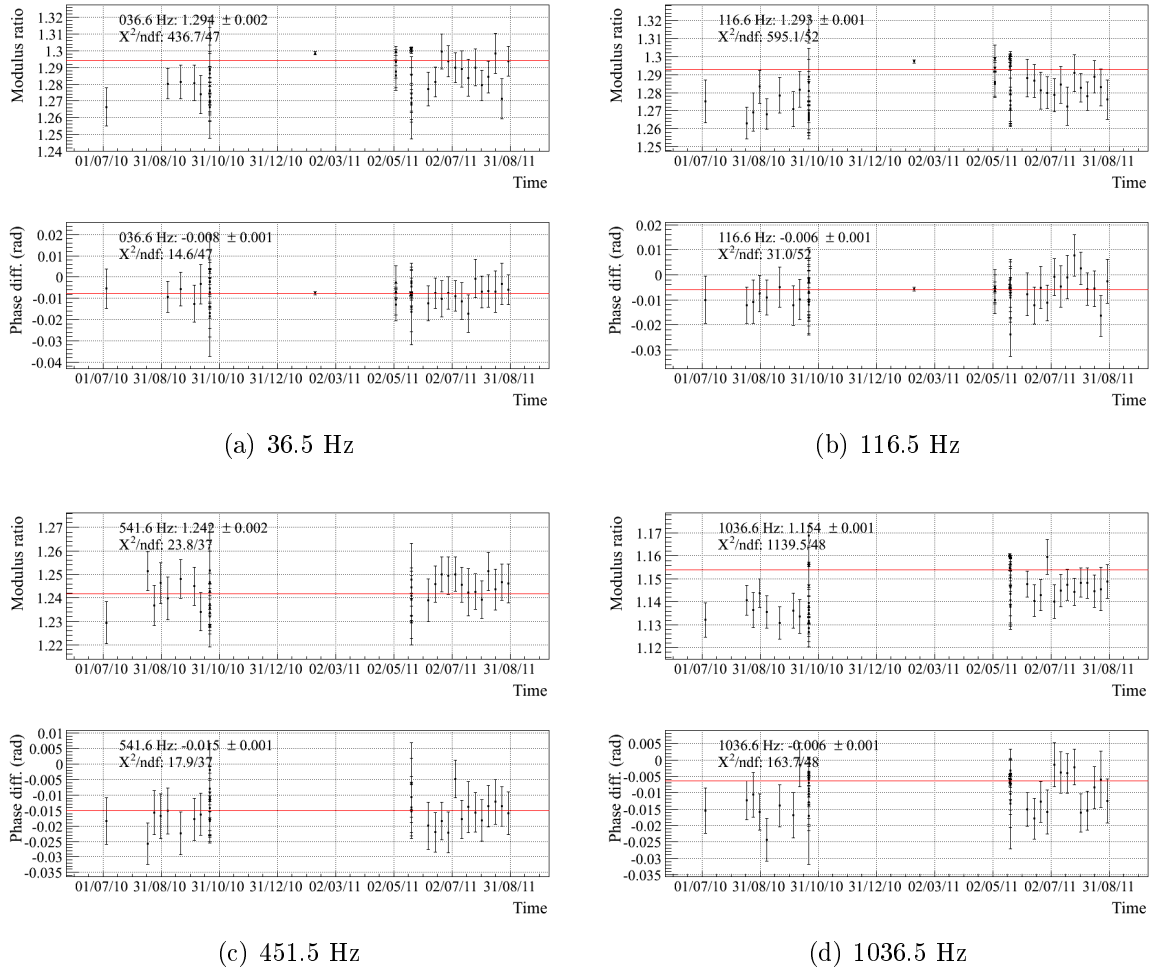
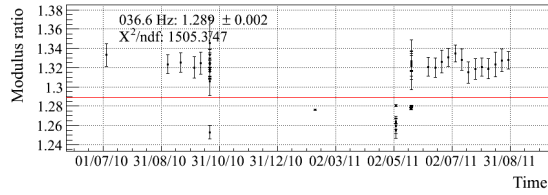
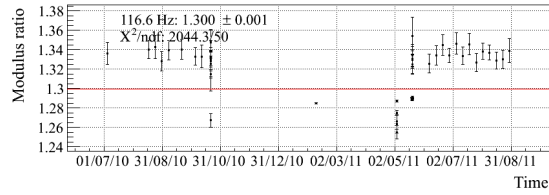
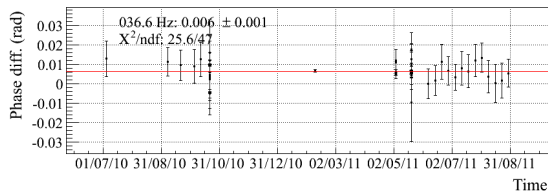


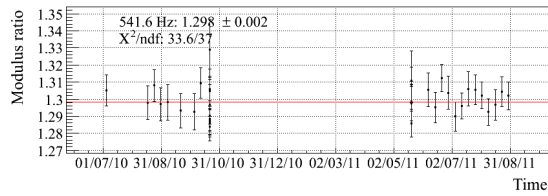
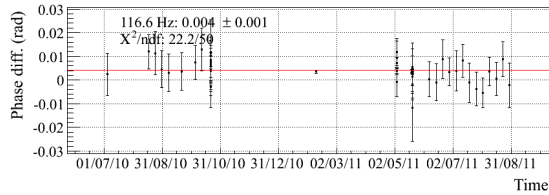
Figure 16: Evolution as function of time (June 2010 to September 2011) of the measured actuation TF ratio (LN1/HP) for the left coil of the WE mirror at four different frequencies.



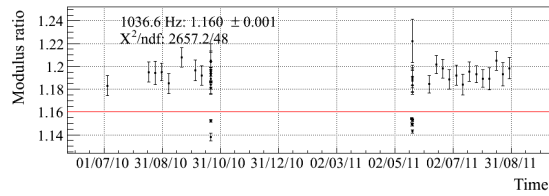
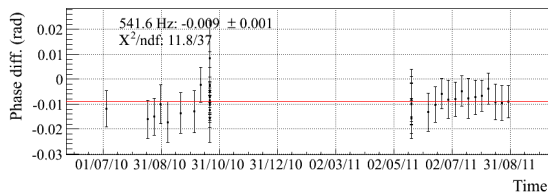
(a) 36.5 Hz



(b) 116.5 Hz



(c) 451.5 Hz



(d) 1036.5 Hz

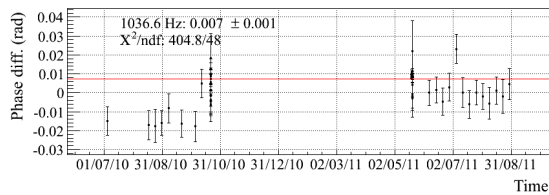


Figure 17: Evolution as function of time (June 2010 to September 2011) of the measured actuation TF ratio (LN1/HP) for the right coil of the WE mirror at four different frequencies.

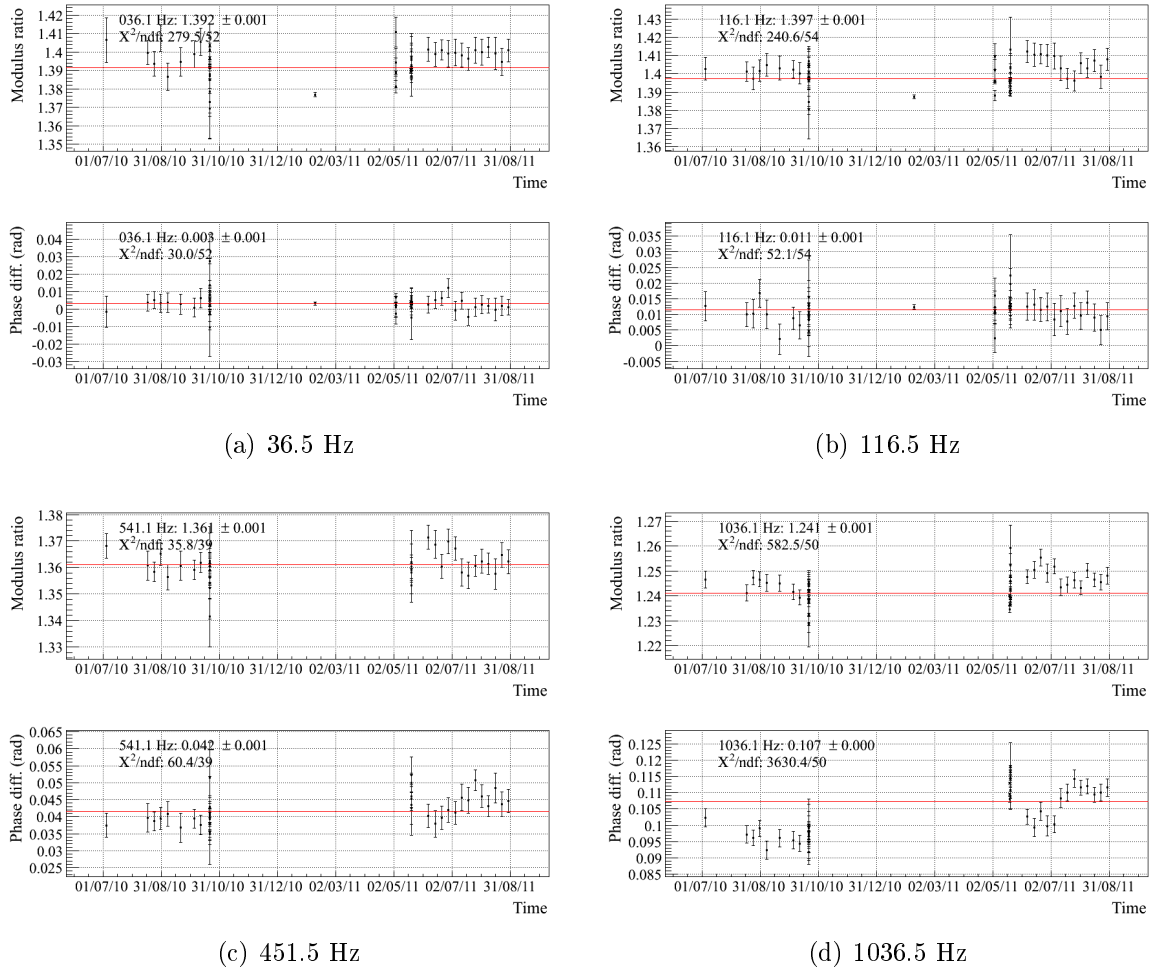


Figure 18: Evolution as function of time (June 2010 to September 2011) of the measured actuation TF ratio (LN1/HP) for the up coil of the NE mirror at four different frequencies.

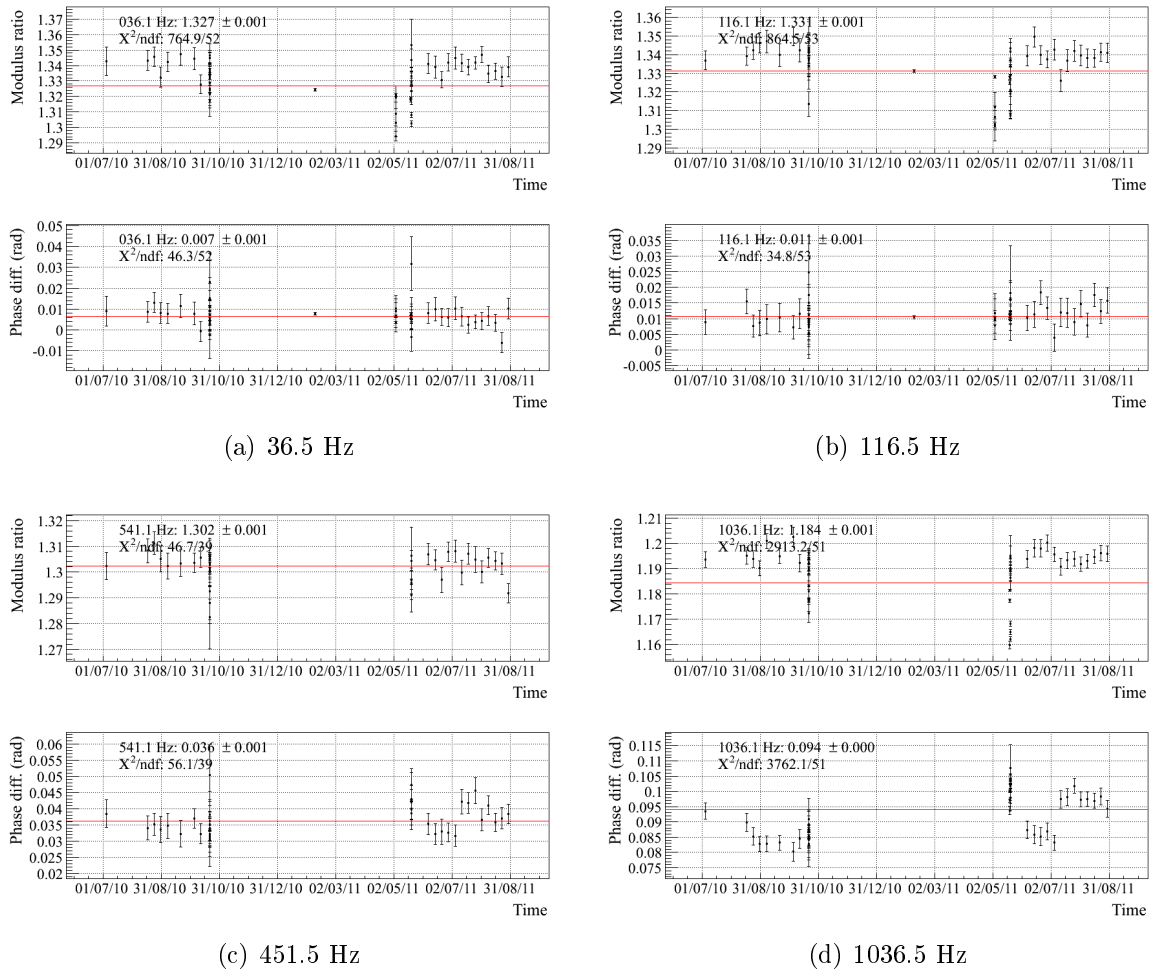


Figure 19: Evolution as function of time (June 2010 to September 2011) of the measured actuation TF ratio (LN1/HP) for the down coil of the NE mirror at four different frequencies.

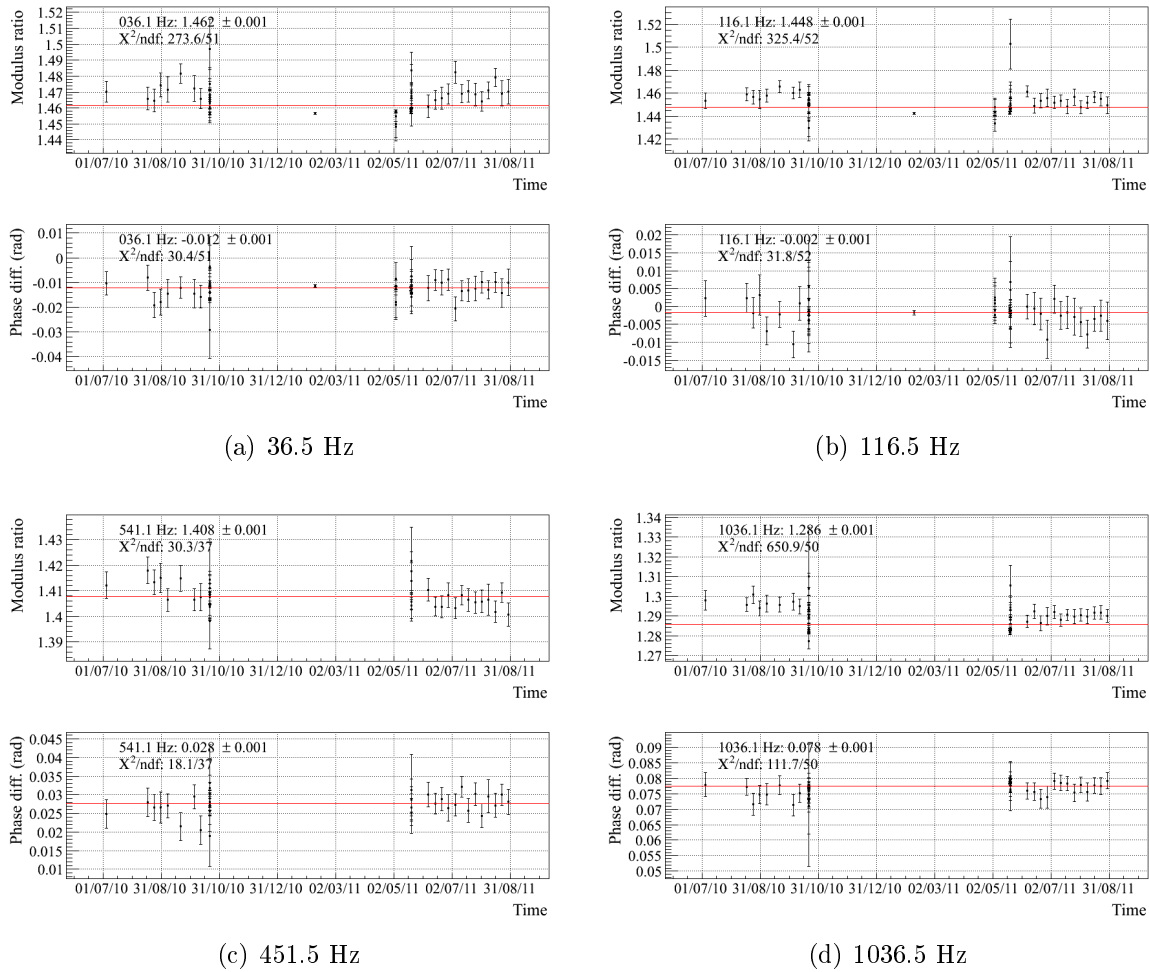
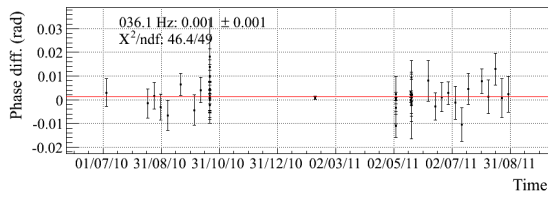
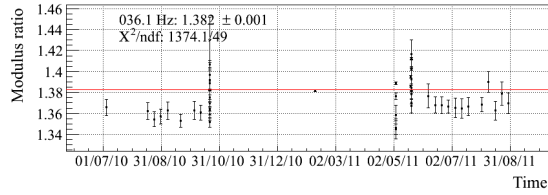
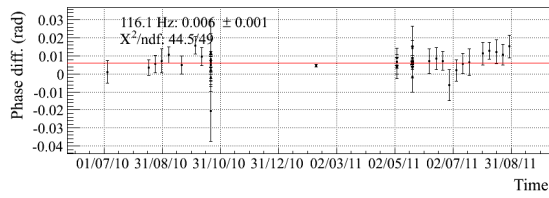
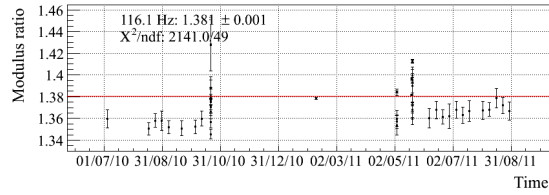


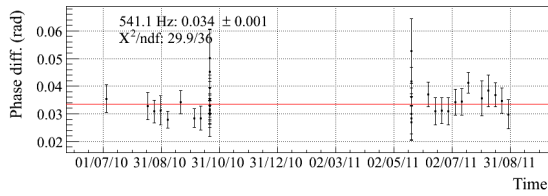
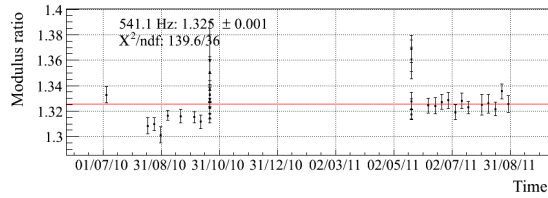
Figure 20: Evolution as function of time (June 2010 to September 2011) of the measured actuation TF ratio (LN1/HP) for the left coil of the NE mirror at four different frequencies.



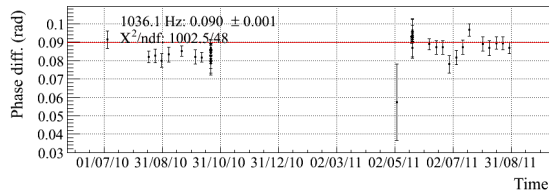
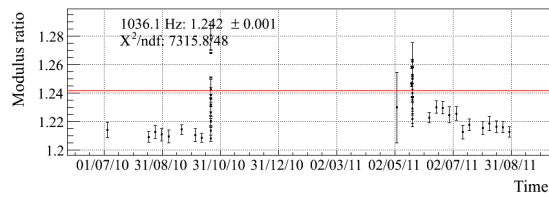
(a) 36.5 Hz



(b) 116.5 Hz



(c) 451.5 Hz



(d) 1036.5 Hz

Figure 21: Evolution as function of time (June 2010 to September 2011) of the measured actuation TF ratio (LN1/HP) for the right coil of the NE mirror at four different frequencies.

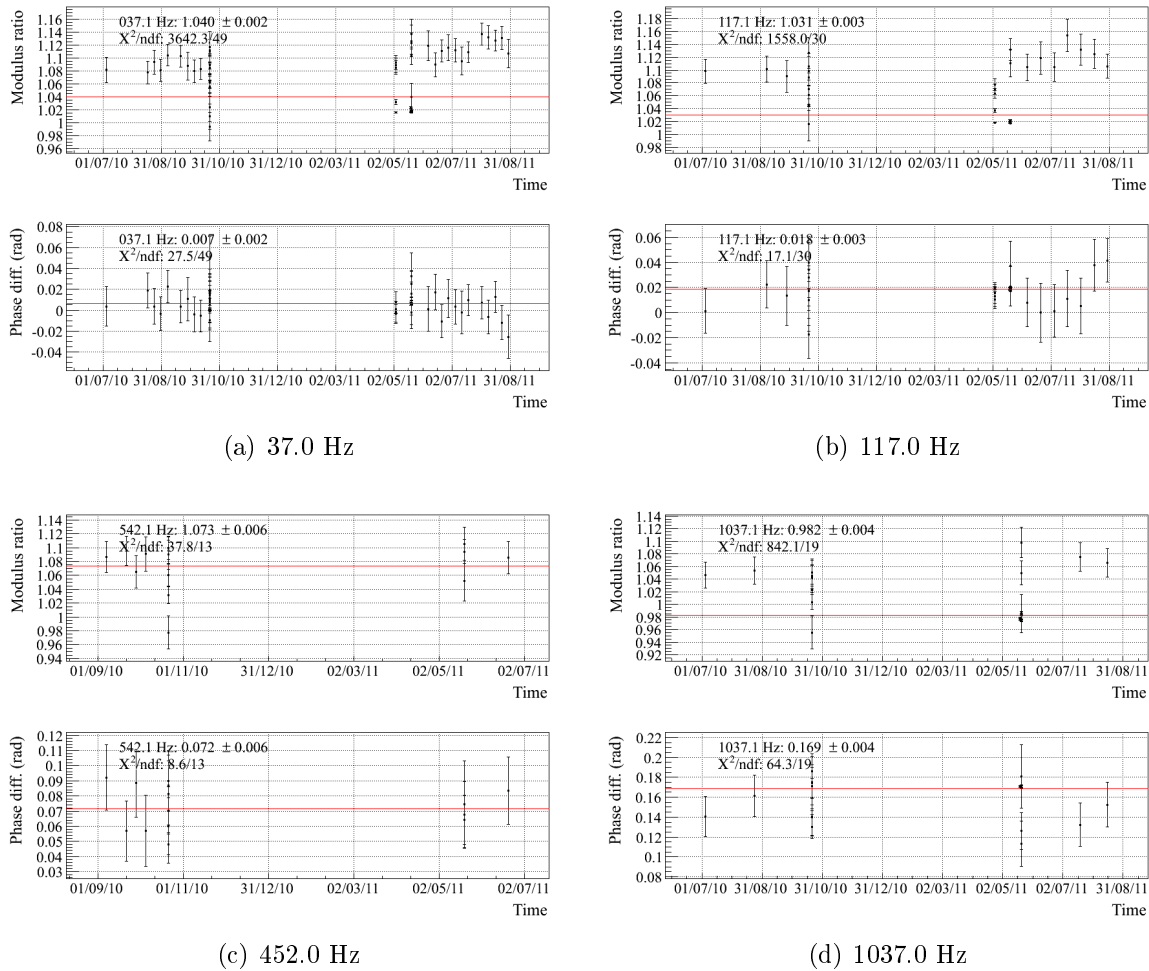
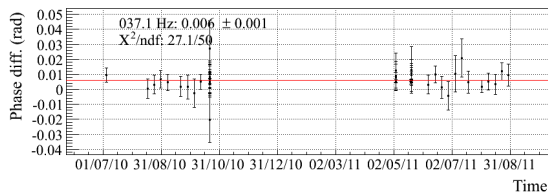
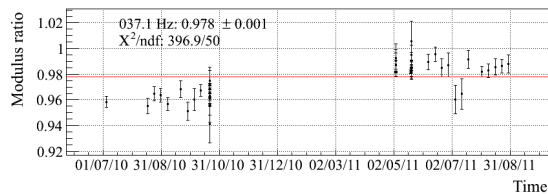
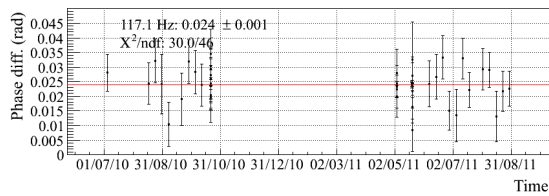
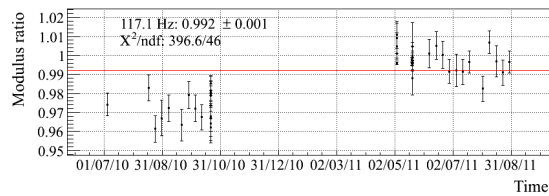


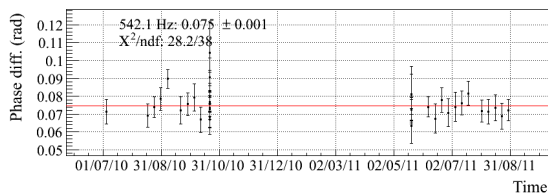
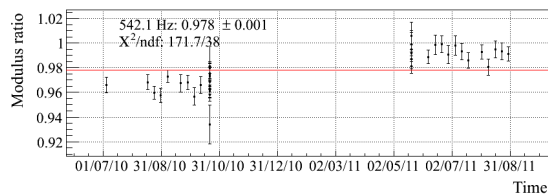
Figure 22: Evolution as function of time (June 2010 to September 2011) of the measured actuation TF ratio (LN1/HP) for the up-left coil of the BS mirror at four different frequencies.



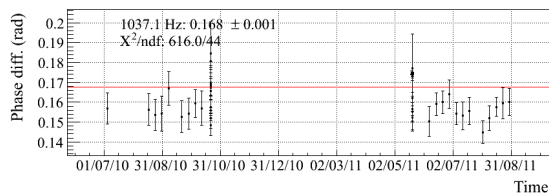
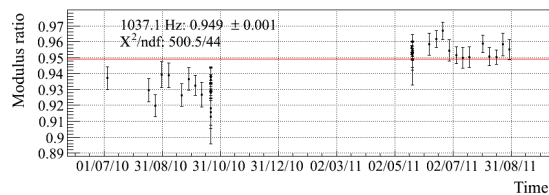
(a) 37.0 Hz



(b) 117.0 Hz

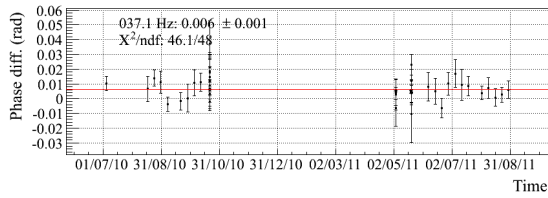
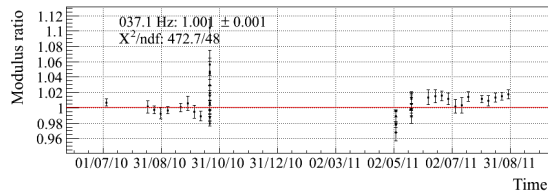


(c) 452.0 Hz

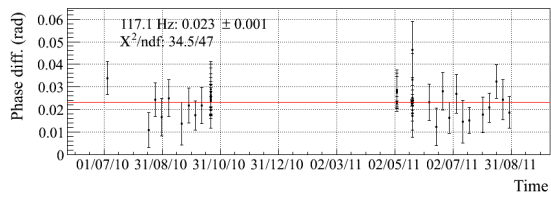
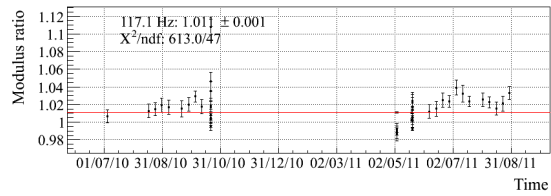


(d) 1037.0 Hz

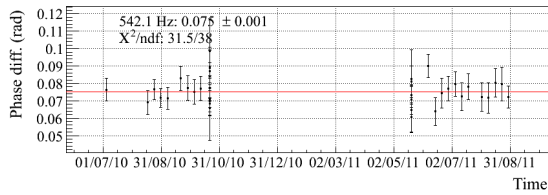
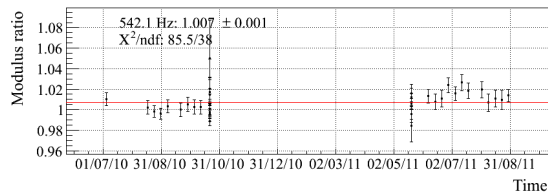
Figure 23: Evolution as function of time (June 2010 to September 2011) of the measured actuation TF ratio (LN1/HP) for the up-right coil of the BS mirror at four different frequencies.



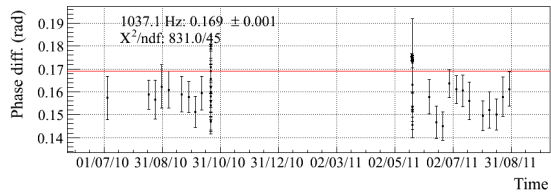
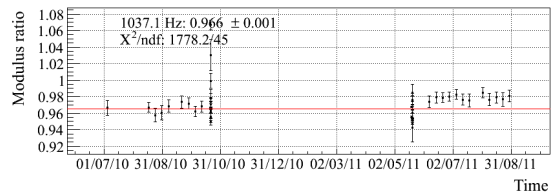
(a) 37.0 Hz



(b) 117.0 Hz



(c) 452.0 Hz



(d) 1037.0 Hz

Figure 24: Evolution as function of time (June 2010 to September 2011) of the measured actuation TF ratio ($LN1/HP$) for the down-left coil of the BS mirror at four different frequencies.

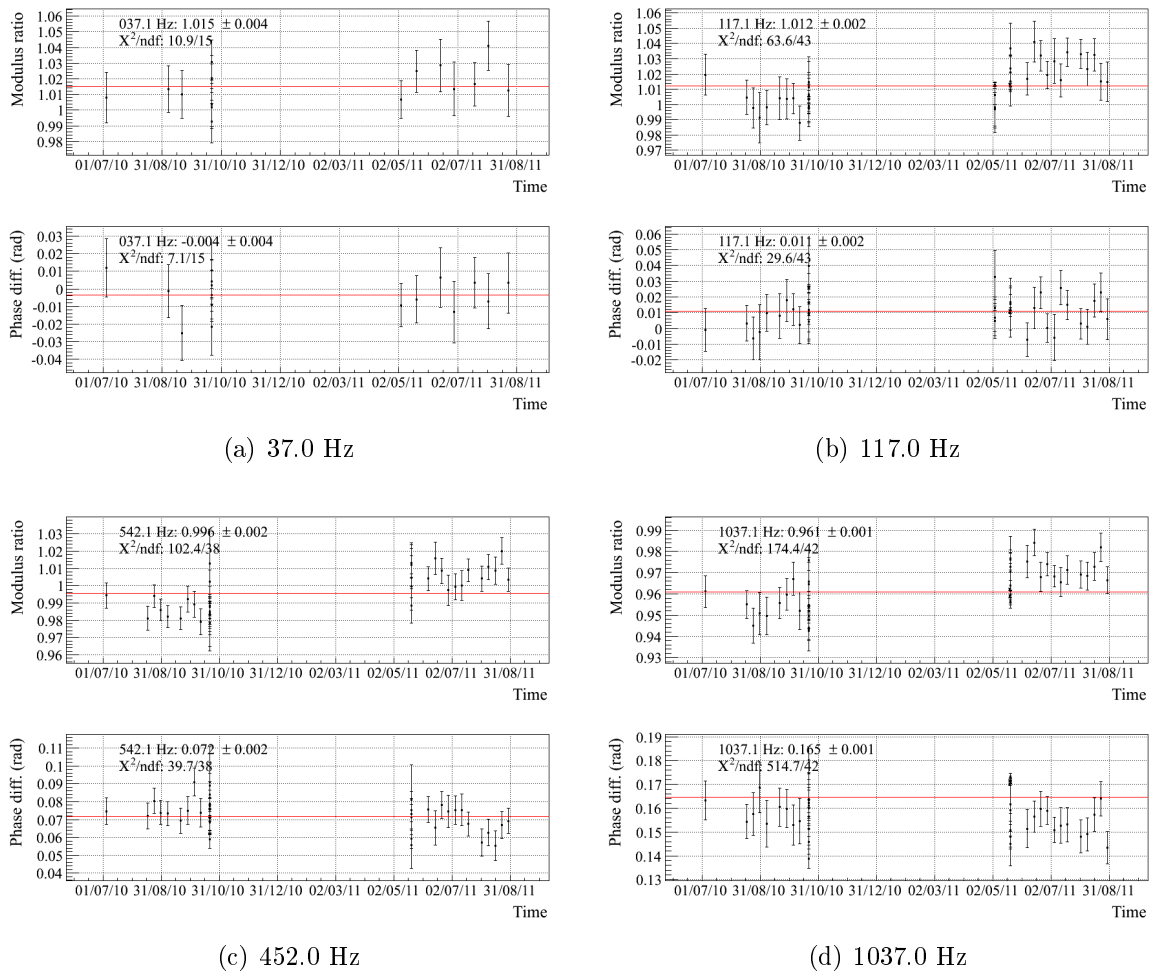


Figure 25: Evolution as function of time (June 2010 to September 2011) of the measured actuation TF ratio (LN1/HP) for the down-right coil of the BS mirror at four different frequencies.

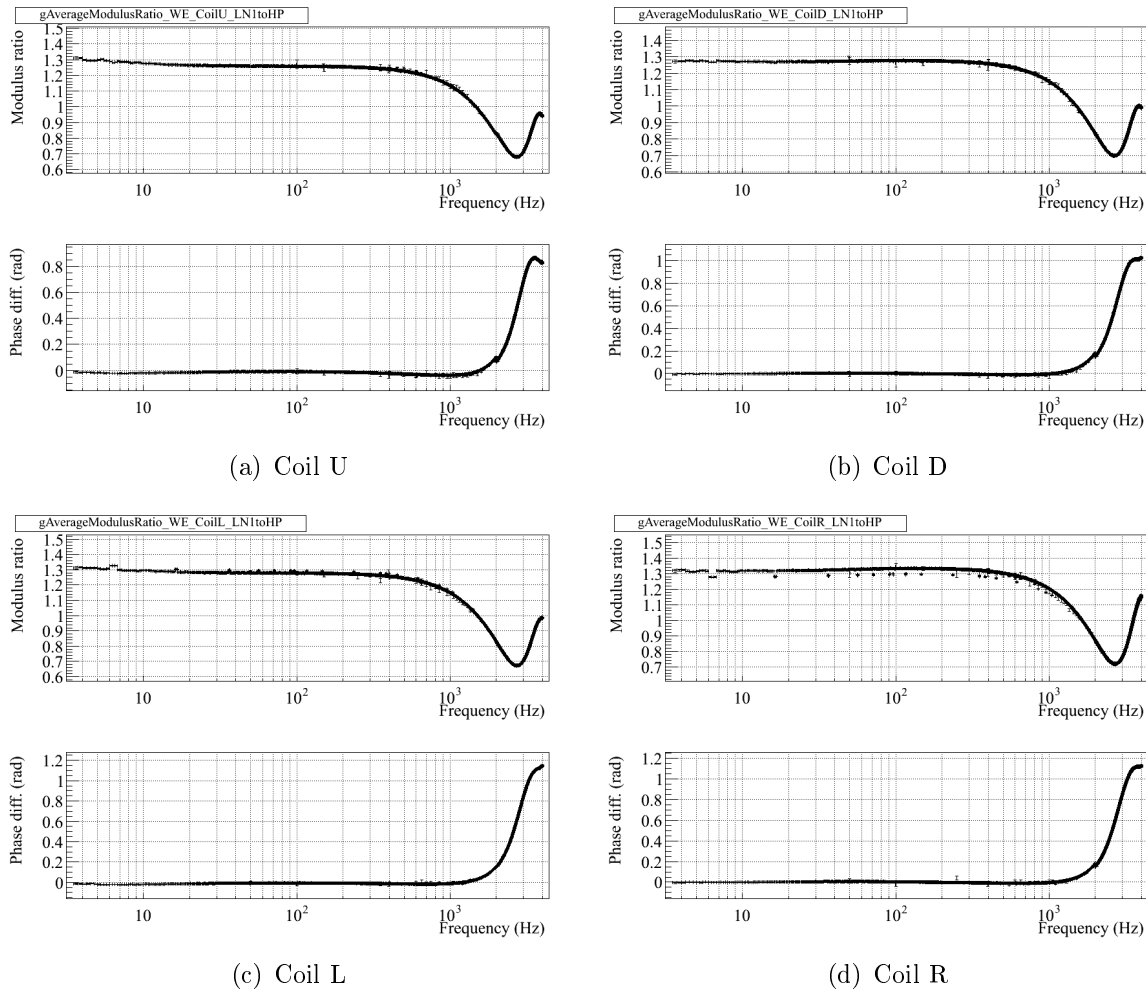
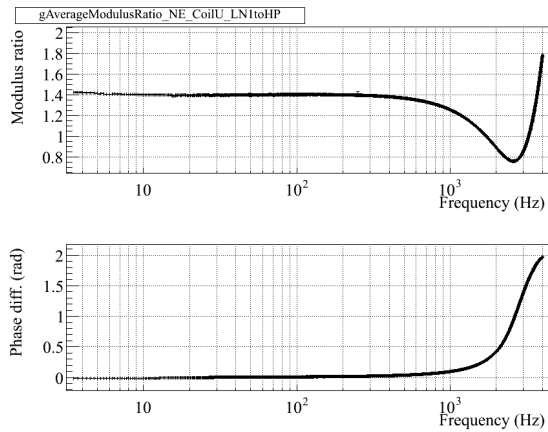
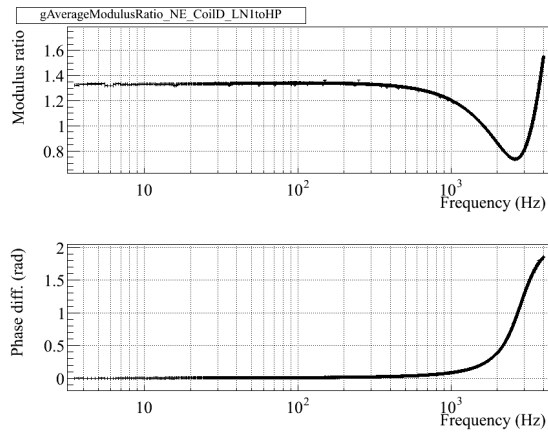


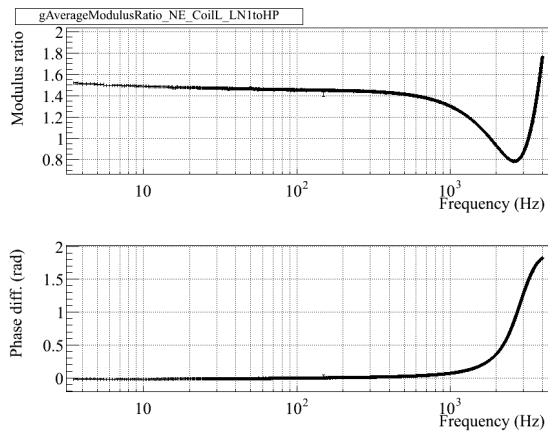
Figure 26: *Averaged LN1/HP ratio of the WE coils (using measurements from June 2010 to September 2011).*



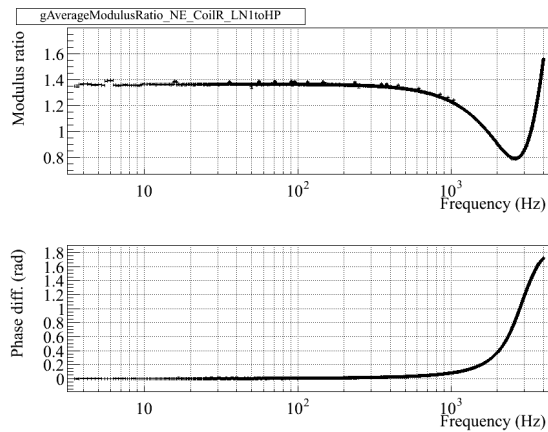
(a) Coil U



(b) Coil D

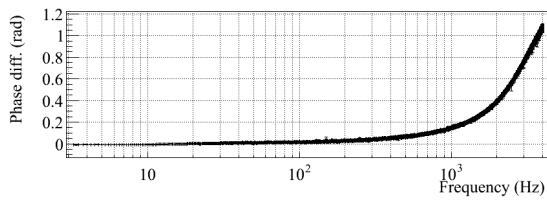
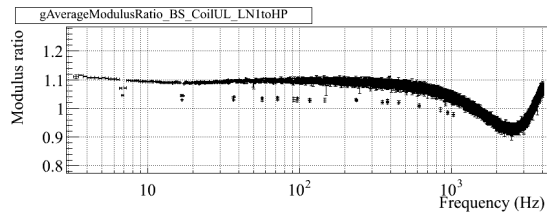


(c) Coil L

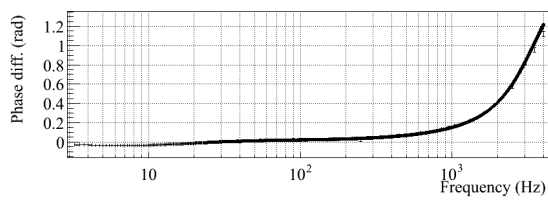
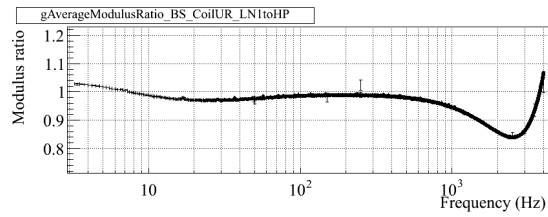


(d) Coil R

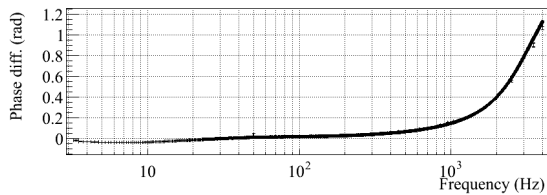
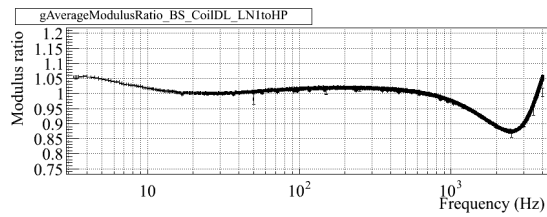
Figure 27: Averaged LN1/HP ratio of the NE coils (using measurements from June 2010 to September 2011).



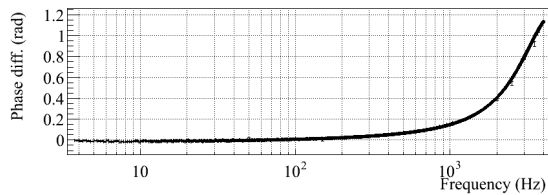
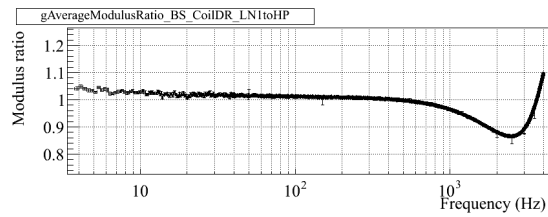
(a) Coil UL



(b) Coil UR



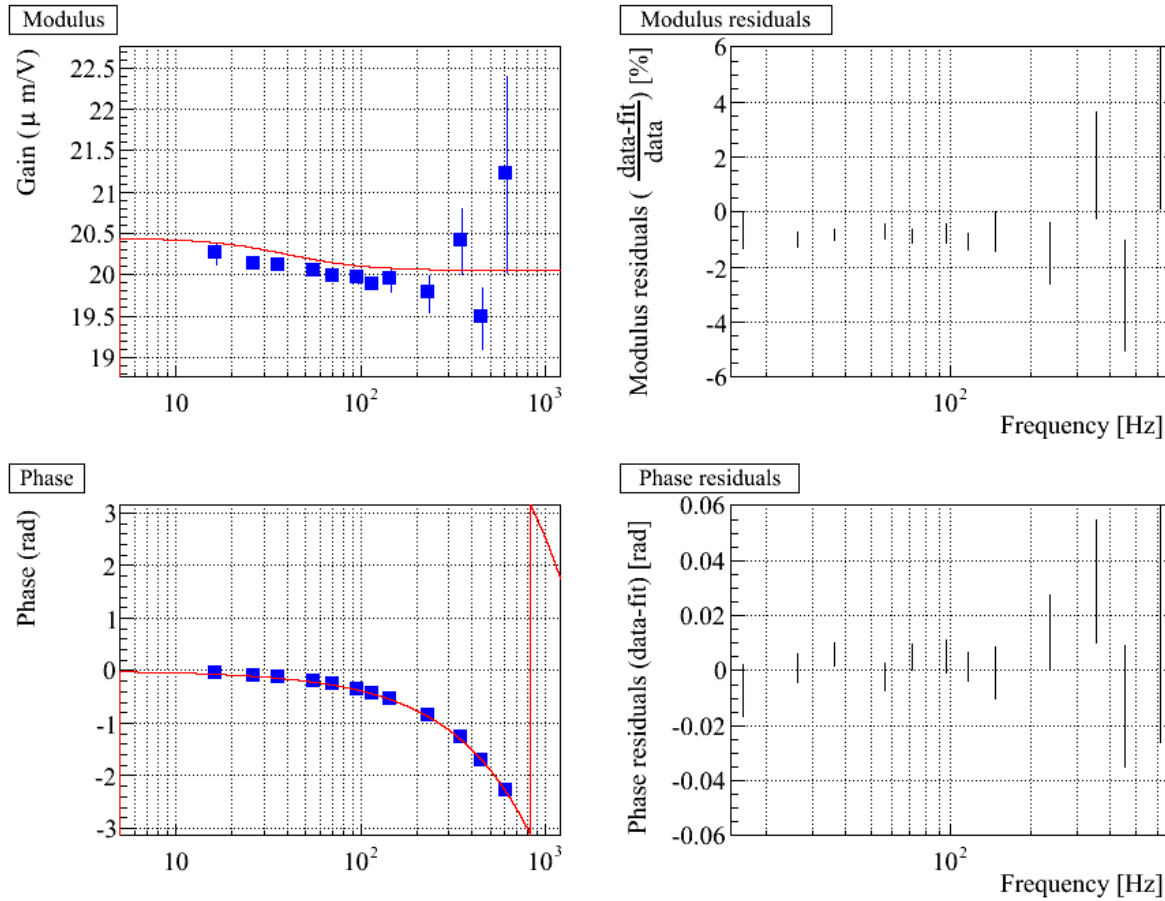
(c) Coil DL



(d) Coil DR

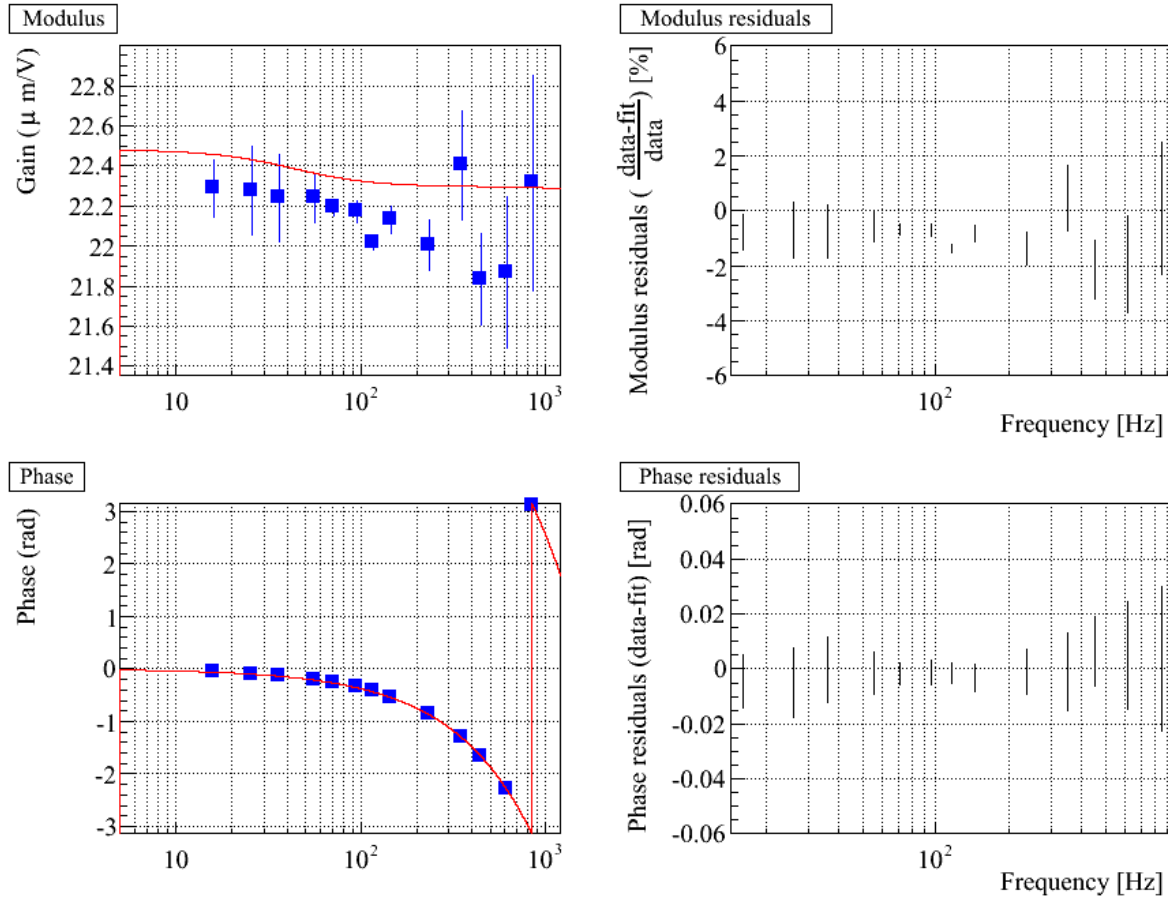
Figure 28: Averaged LN1/HP ratio of the BS coils (using measurements from June 2010 to September 2011).

A.2.2 Comparison of VSR3 parameterization with latest data



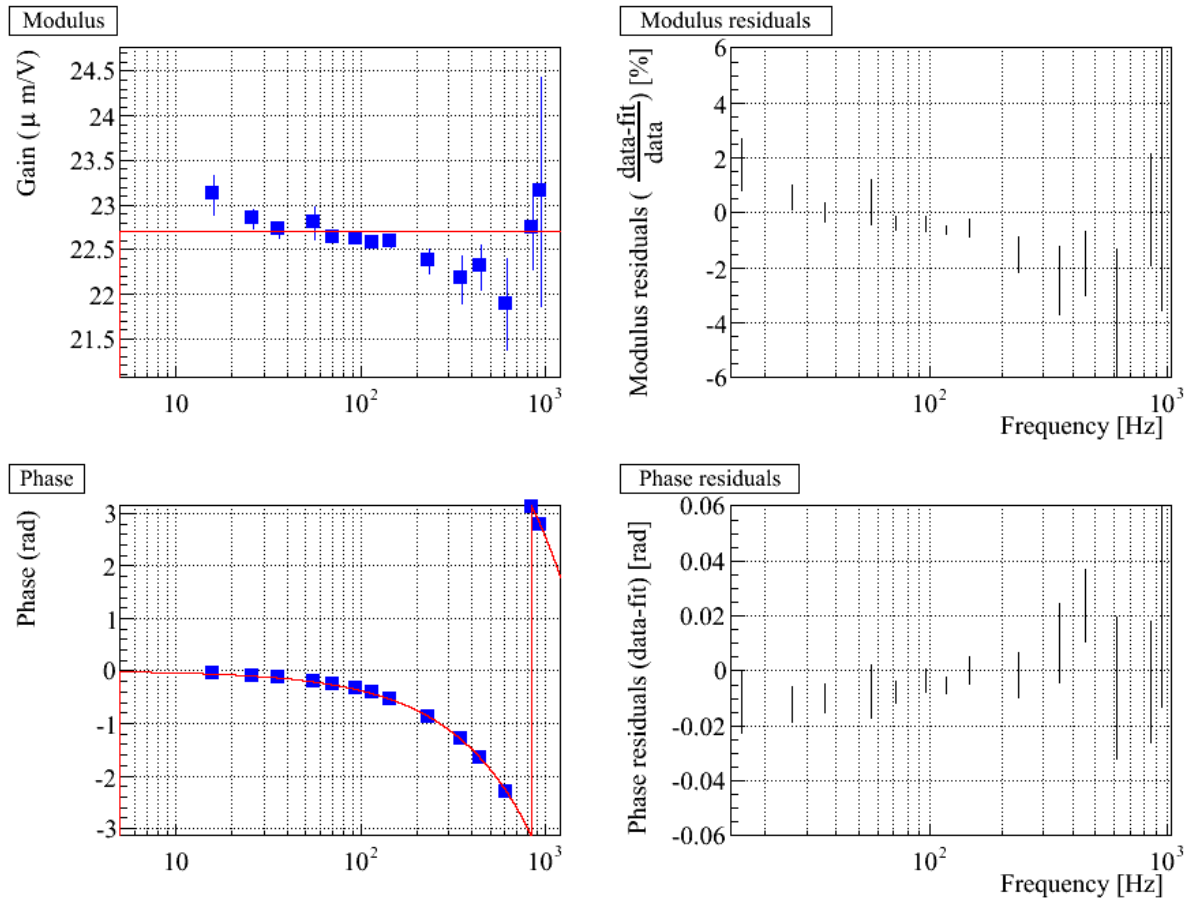
(a) WE, L-R

Figure 29: WE, L-R mirror actuation in LN1 mode. Left: comparison of VSR3 model (red) with VSR4 averaged measurements (blue). Right: residuals.



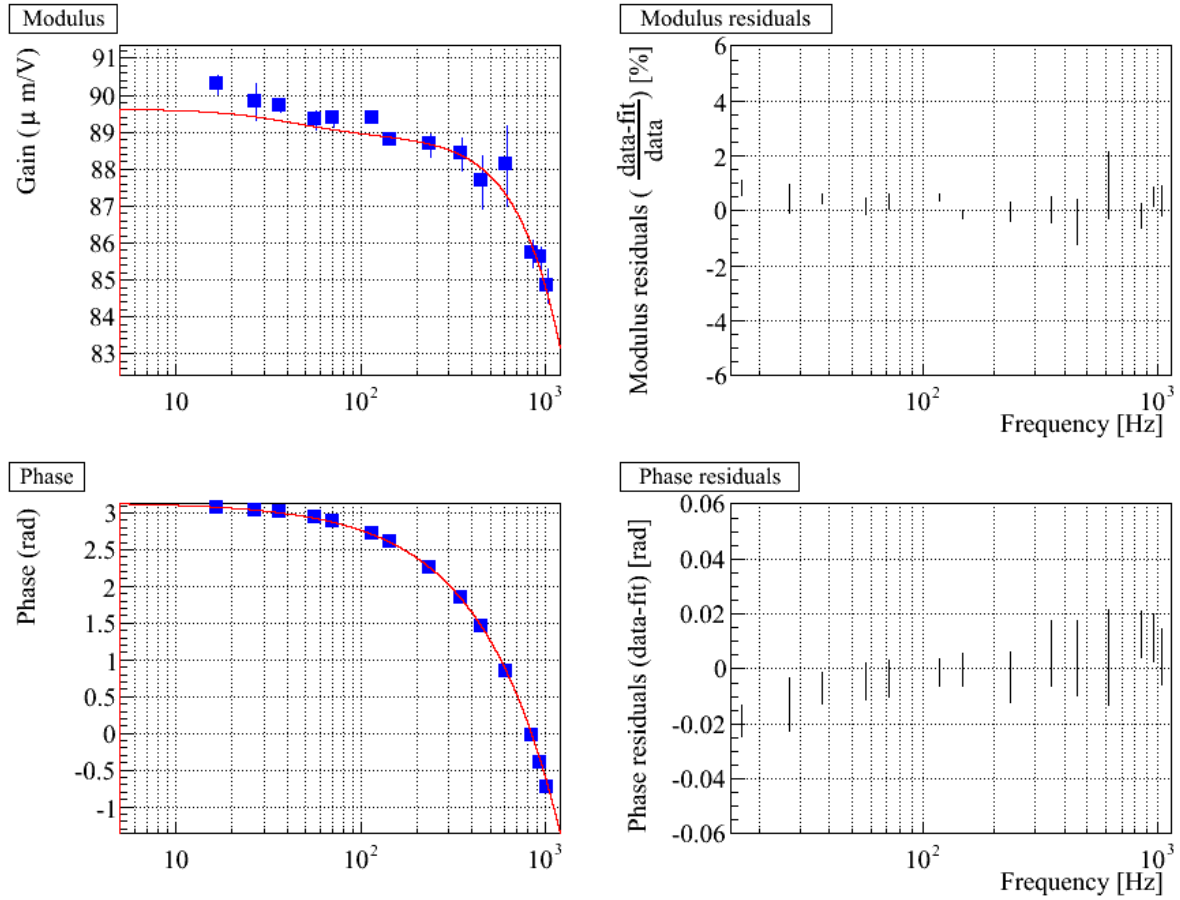
(a) NE, U-D

Figure 30: *NE, U-D mirror actuation in LN1 mode. Left: comparison of VSR3 model (red) with VSR4 averaged measurements (blue). Right: residuals.*



(a) NE, L-R

Figure 31: NE, L-R mirror actuation in LN1 mode. Left: comparison of VSR3 model (red) with VSR4 averaged measurements (blue). Right: residuals.

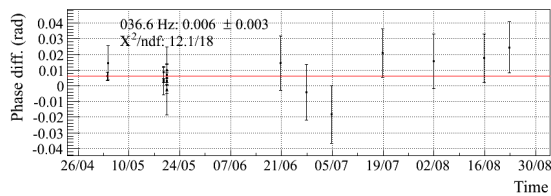
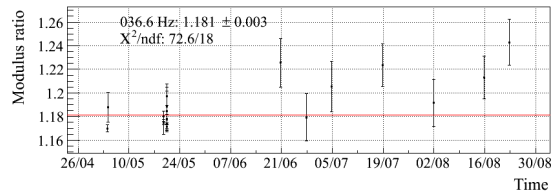


(a) BS, 4 coils

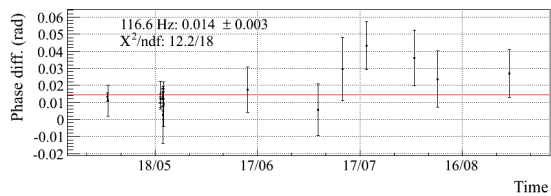
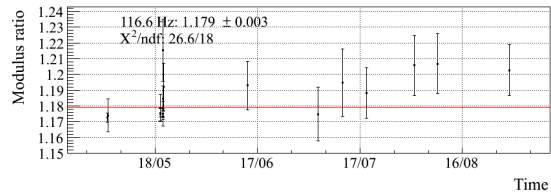
Figure 32: *BS mirror actuation in LN1 mode. Left: comparison of VSR3 model (red) with VSR4 averaged measurements (blue). Right: residuals.*

A.3 LN2/HP ratio

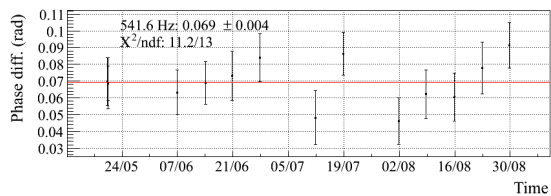
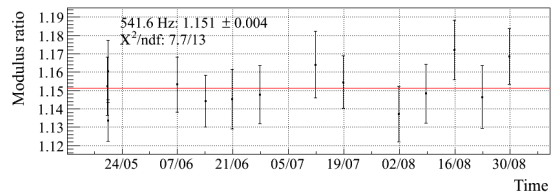
A.3.1 LN2/HP stability (May to September 2011)



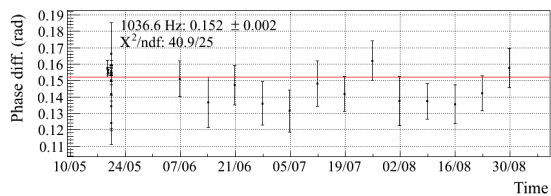
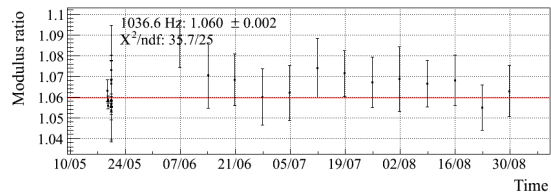
(a) 36.5 Hz



(b) 116.5 Hz



(c) 451.5 Hz



(d) 1036.5 Hz

Figure 33: Evolution as function of time (June 2010 to May 2011) of the measured actuation TF ratio (LN2/HP) for the down coil of the WE mirror at four different frequencies.

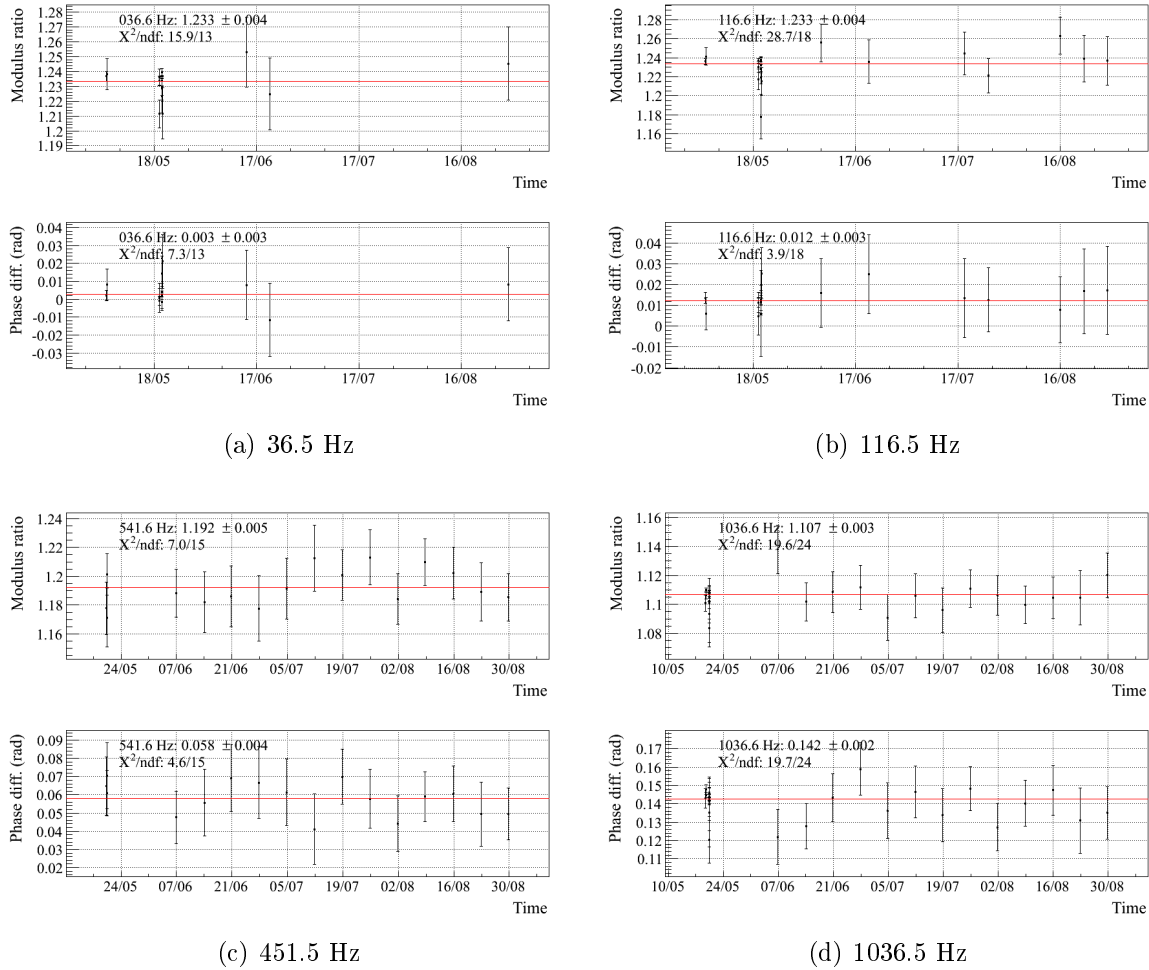


Figure 34: Evolution as function of time (June 2010 to May 2011) of the measured actuation TF ratio (LN2/HP) for the left coil of the WE mirror at four different frequencies.

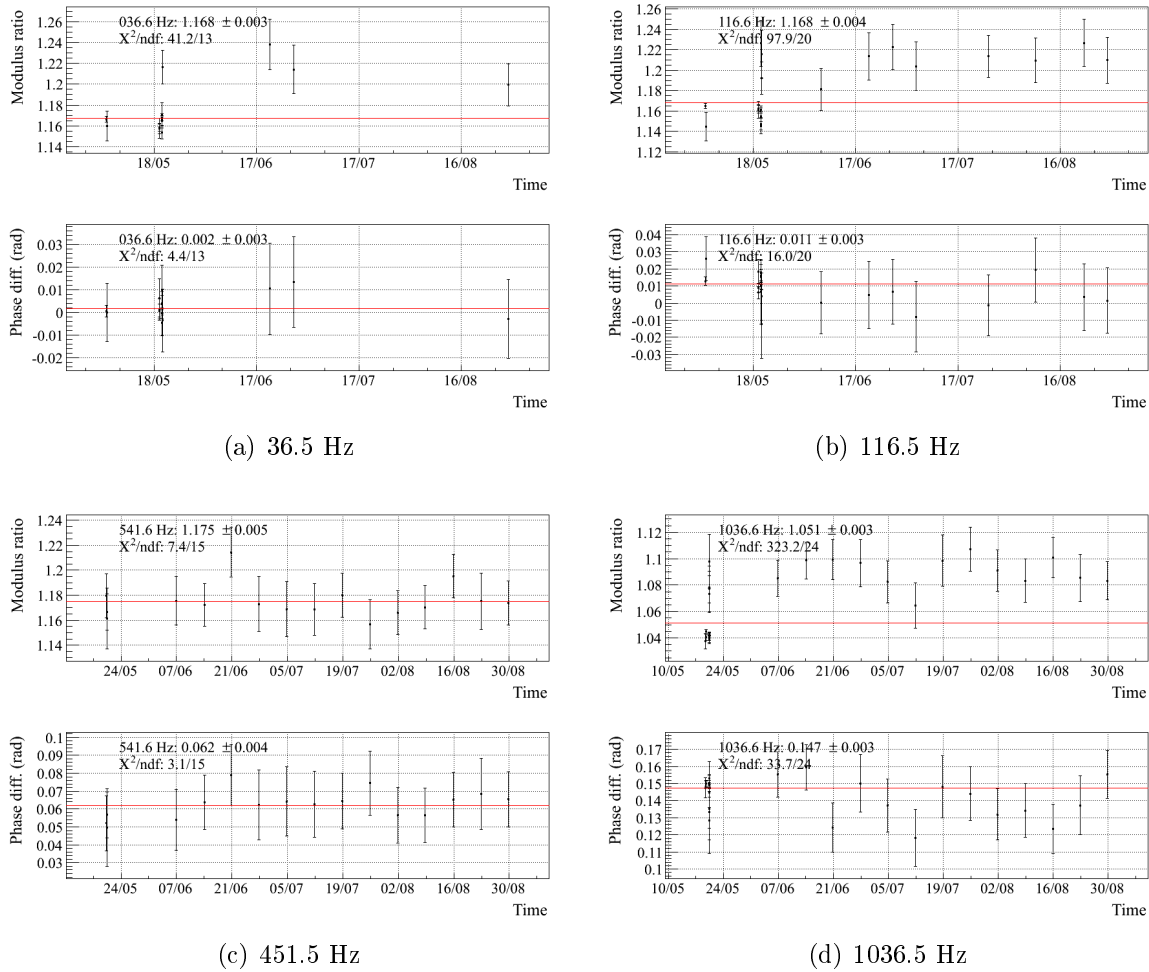
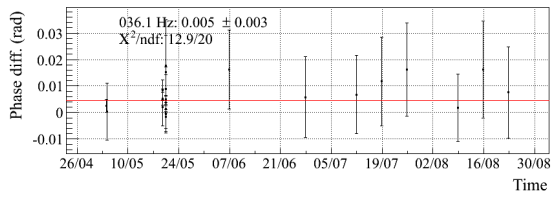
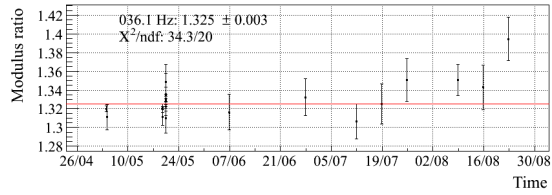
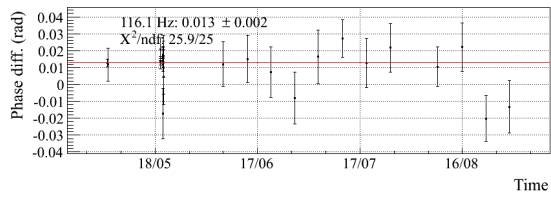
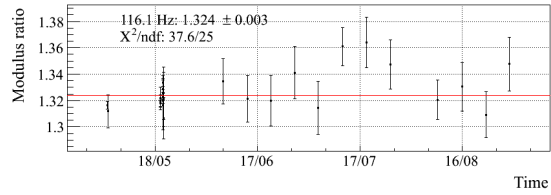


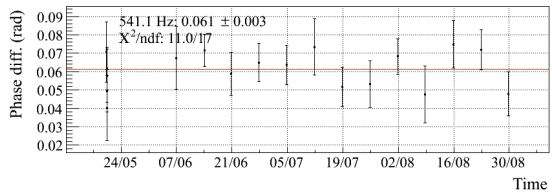
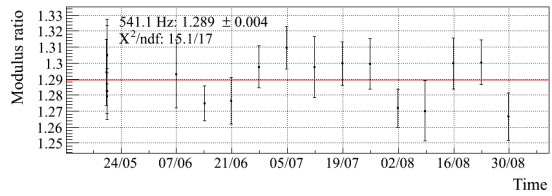
Figure 35: Evolution as function of time (June 2010 to May 2011) of the measured actuation TF ratio (LN2/HP) for the right coil of the WE mirror at four different frequencies.



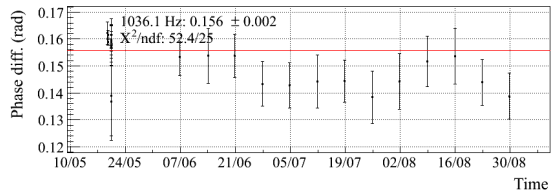
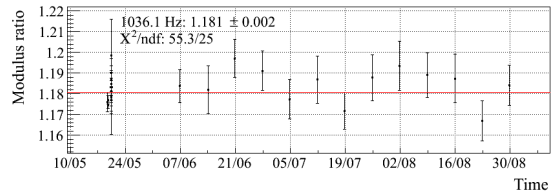
(a) 36.5 Hz



(b) 116.5 Hz

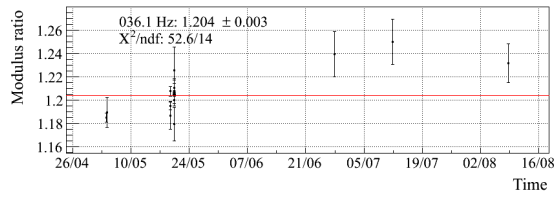


(c) 451.5 Hz

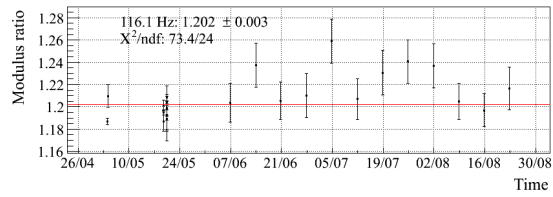


(d) 1036.5 Hz

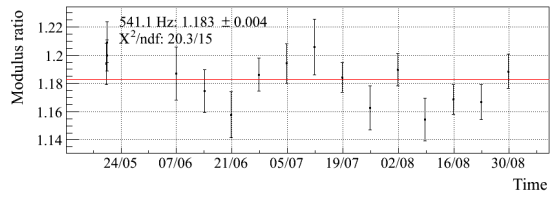
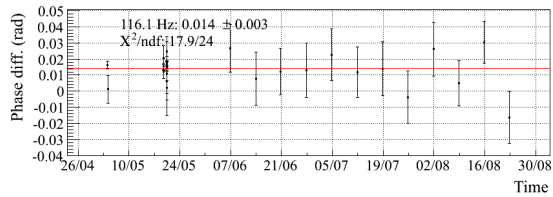
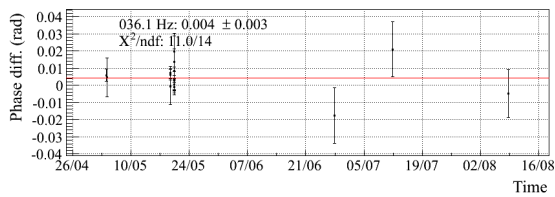
Figure 36: Evolution as function of time (June 2010 to May 2011) of the measured actuation TF ratio ($LN2/HP$) for the up coil of the NE mirror at four different frequencies.



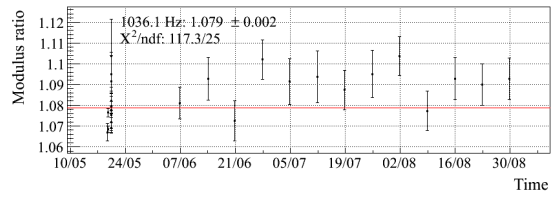
(a) 36.5 Hz



(b) 116.5 Hz



(c) 451.5 Hz



(d) 1036.5 Hz

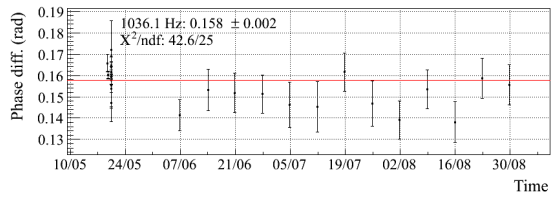
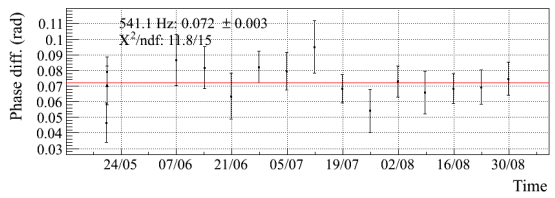
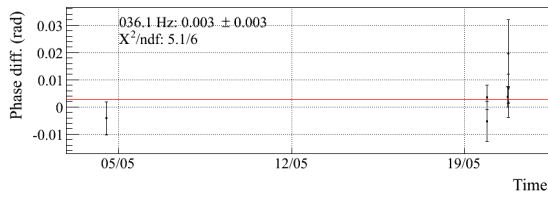
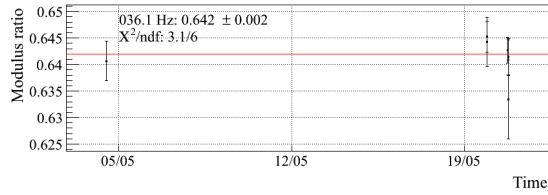
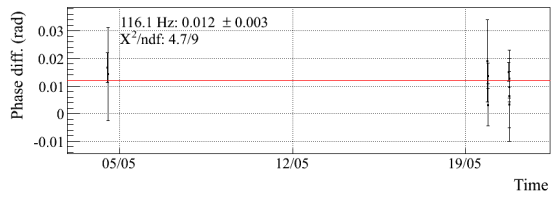
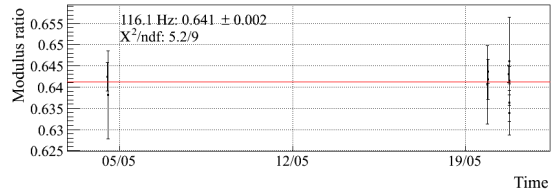


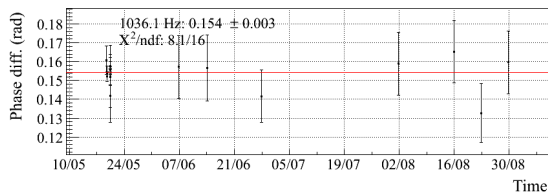
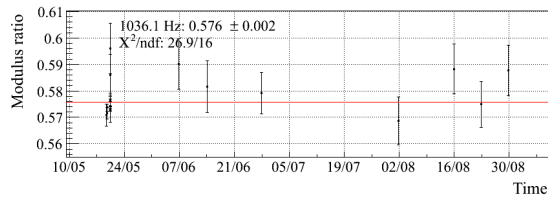
Figure 37: Evolution as function of time (June 2010 to May 2011) of the measured actuation TF ratio (LN2/HP) for the down coil of the NE mirror at four different frequencies.



(a) 36.5 Hz

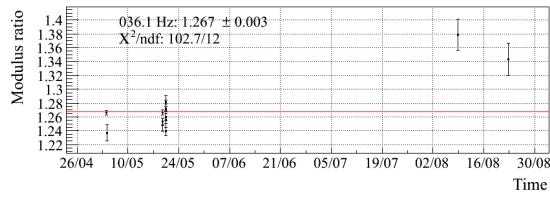


(b) 116.5 Hz

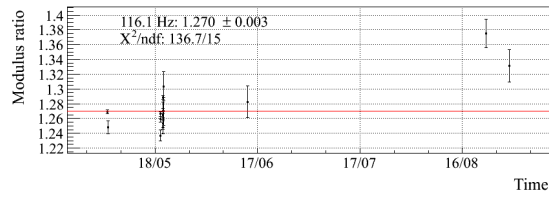


(c) 1036.5 Hz

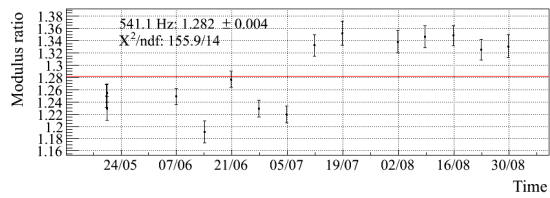
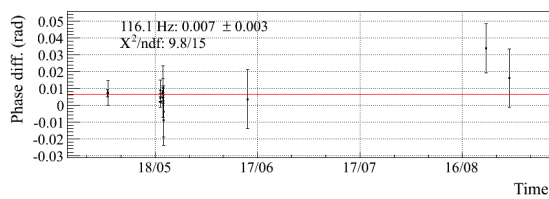
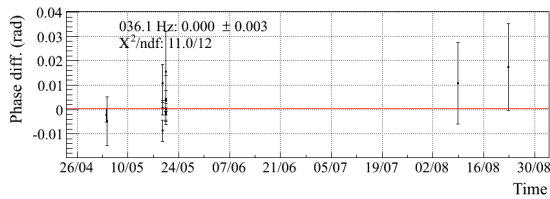
Figure 38: Evolution as function of time (June 2010 to May 2011) of the measured actuation TF ratio ($LN2/HP$) for the left coil of the NE mirror at four different frequencies.



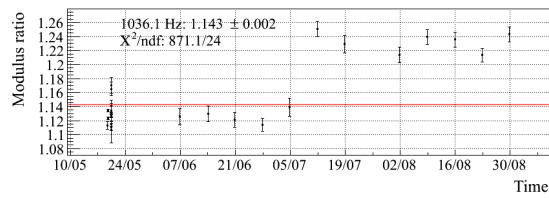
(a) 36.5 Hz



(b) 116.5 Hz



(c) 451.5 Hz



(d) 1036.5 Hz

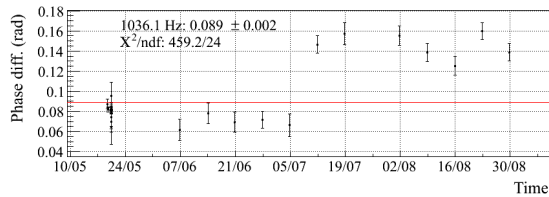
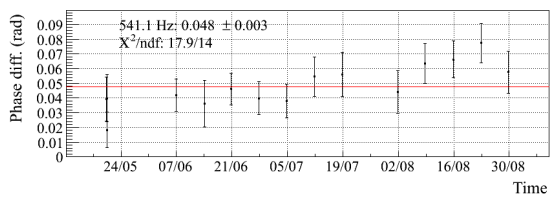


Figure 39: Evolution as function of time (June 2010 to May 2011) of the measured actuation TF ratio (LN2/HP) for the right coil of the NE mirror at four different frequencies.

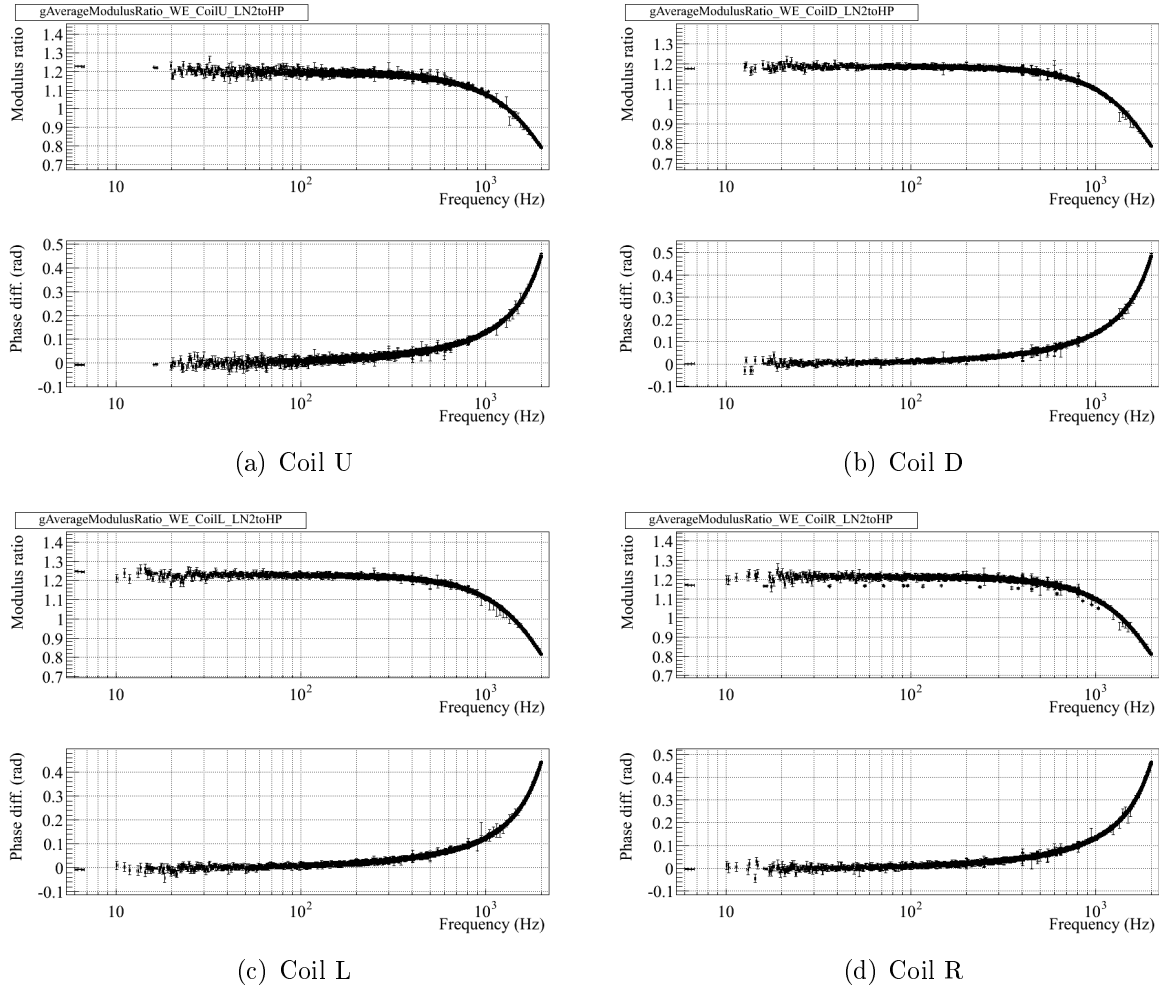
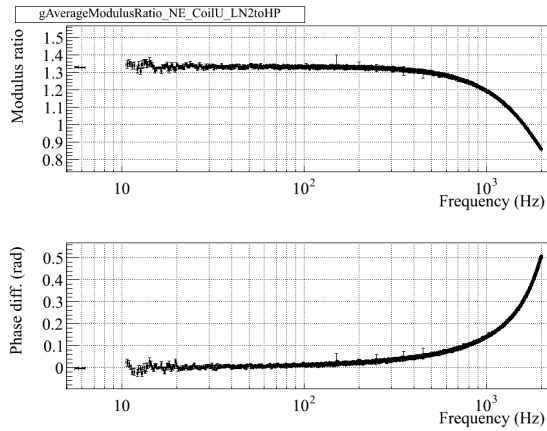
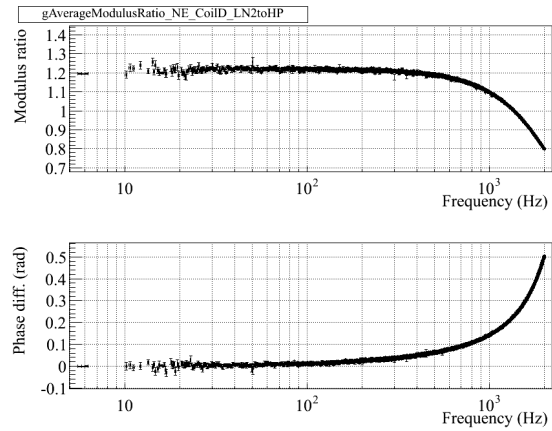


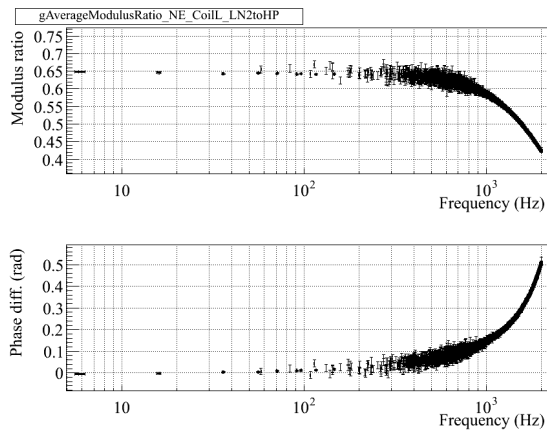
Figure 40: Measured actuation TF ratio (LN2/HP) for the four coils of the WE mirror.



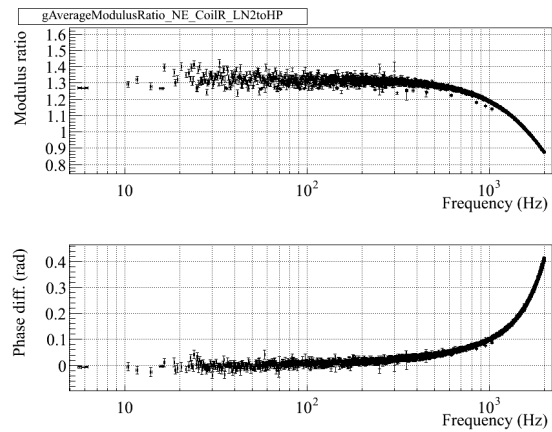
(a) Coil U



(b) Coil D



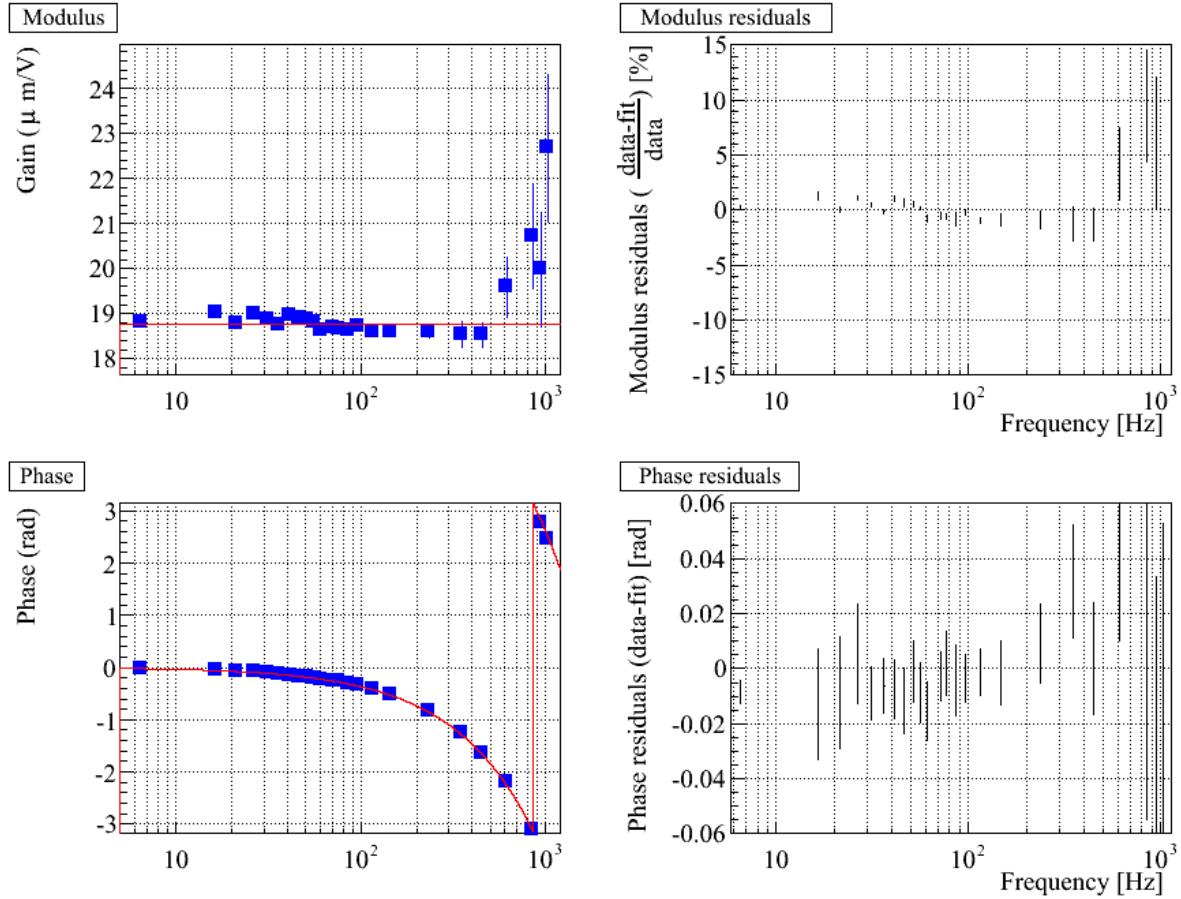
(c) Coil L



(d) Coil R

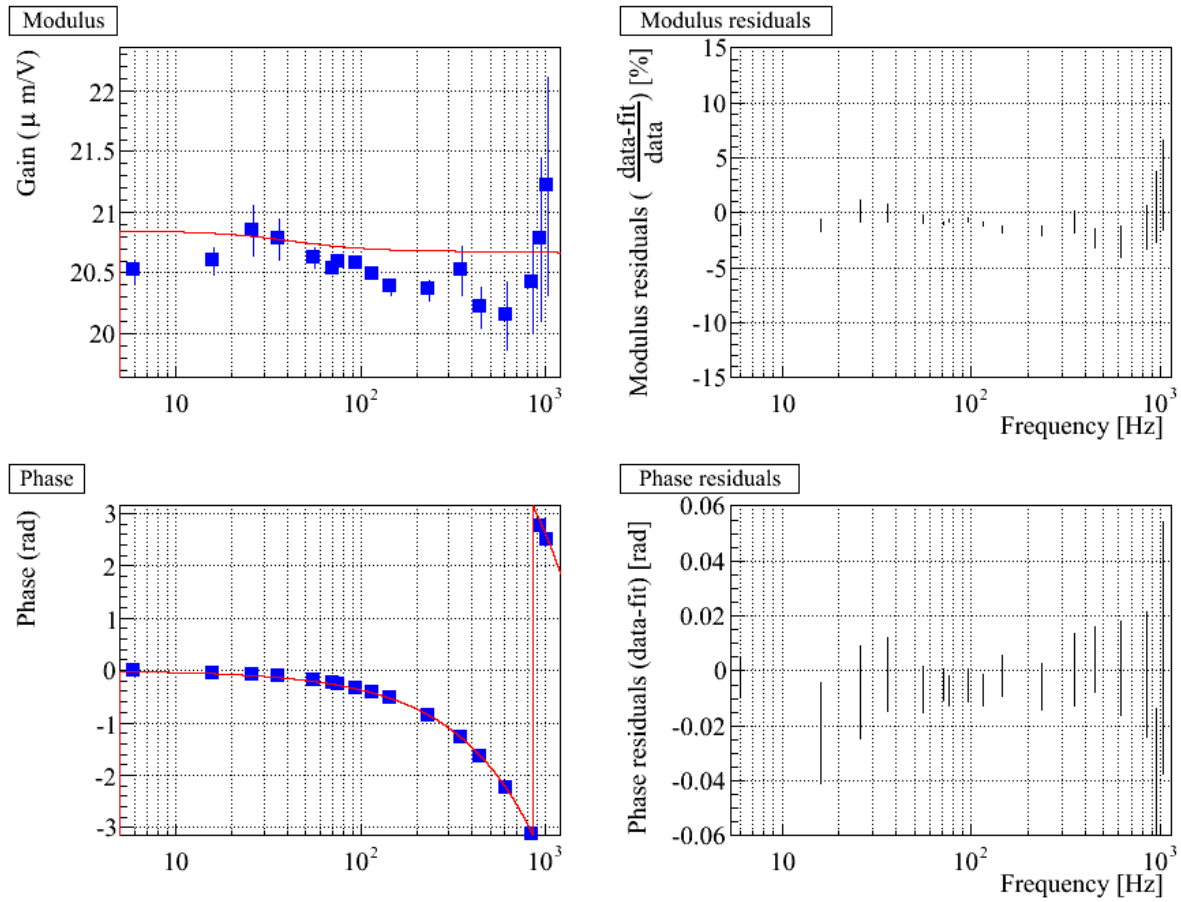
Figure 41: Measured actuation TF ratio (LN2/HP) for the four coils of the NE mirror.

A.3.2 Comparison of the pre-VSR4 parameterization with VSR4 data



(a) WE, L-R

Figure 42: WE, L-R mirror actuation in LN2 mode. Left: comparison of pre-VSR4 model (red) with all VSR4 averaged measurements (blue). Right: residuals.



(a) NE, U-D

Figure 43: NE, U-D mirror actuation in LN2 mode. Left: comparison of pre-VSR4 model (red) with all VSR4 averaged measurements (blue). Right: residuals.

B Appendix: Marionette actuation

B.1 Marionette actuation: evolution (June 2010 to Sept. 2011)

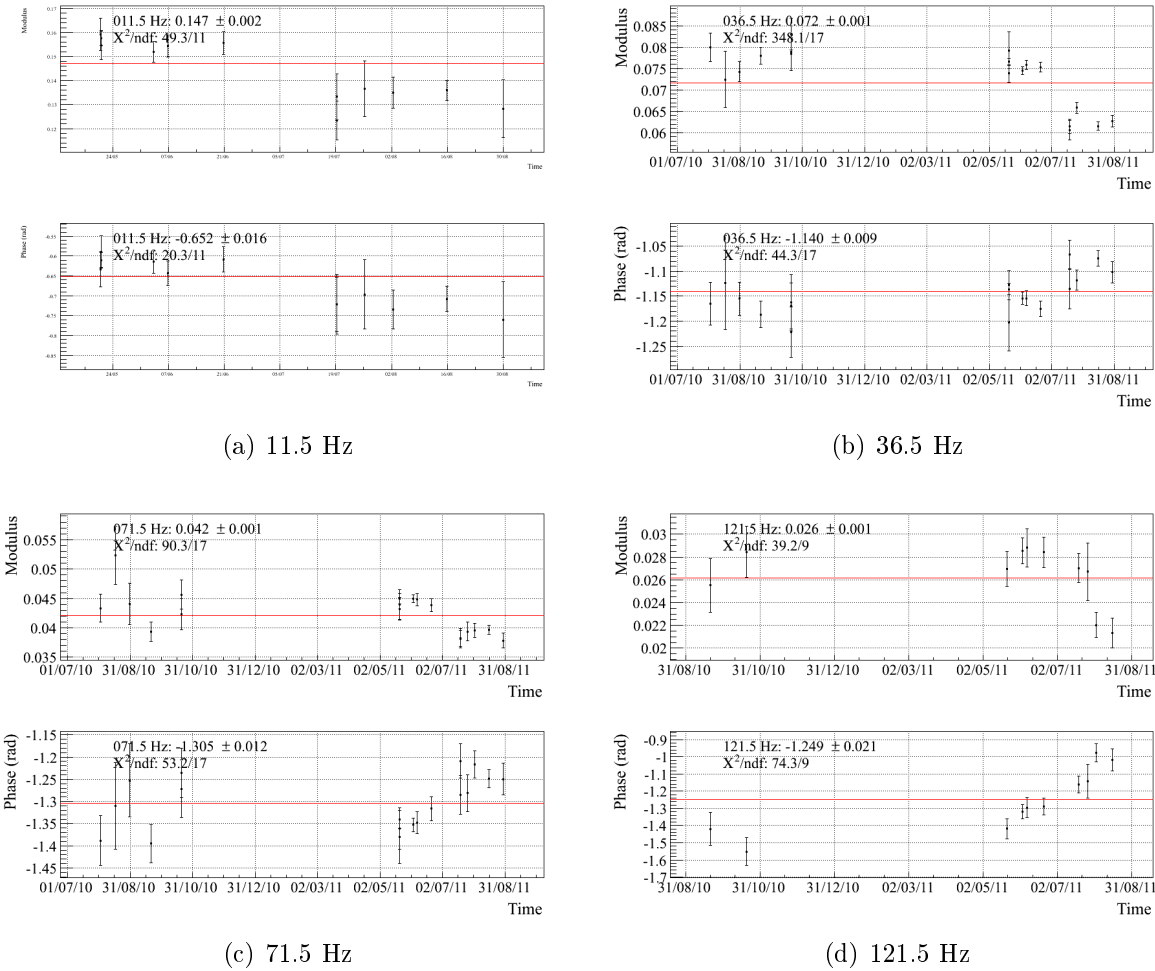
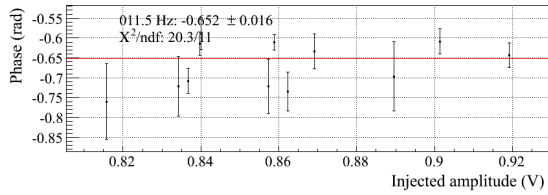
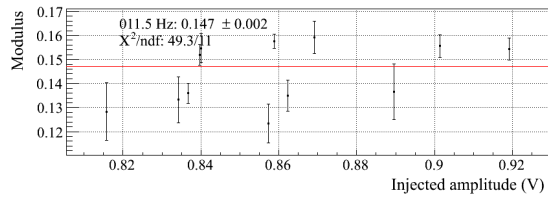
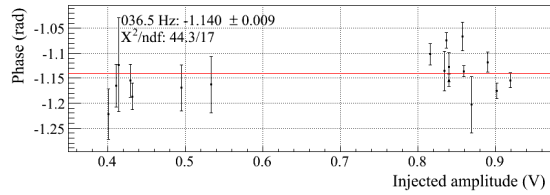
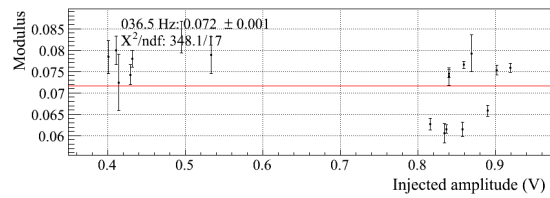


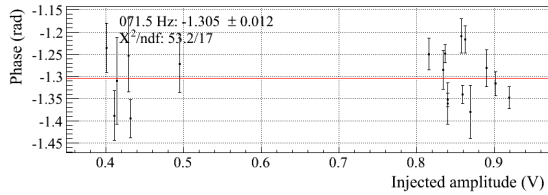
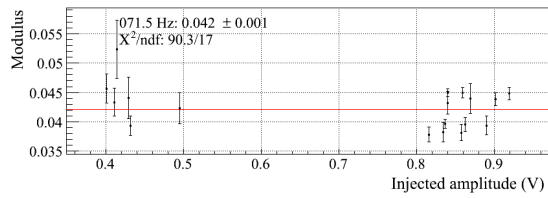
Figure 44: Measured WE marionette to mirror actuation (WE, U-D coils, LN1) TF ratio as function of time at four different frequencies. The mirror and marionette actuations have been corrected for their pendulum mechanical models.



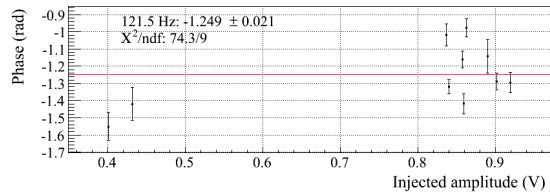
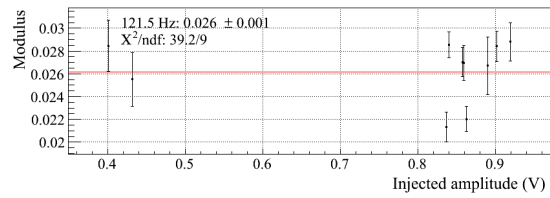
(a) 11.5 Hz



(b) 36.5 Hz



(c) 71.5 Hz



(d) 121.5 Hz

Figure 45: Measured WE marionette to mirror actuation (WE, U-D coils, LN1) TF ratio as function of amplitude of injected noise at four different frequencies. The mirror and marionette actuations have been corrected for their pendulum mechanical models.

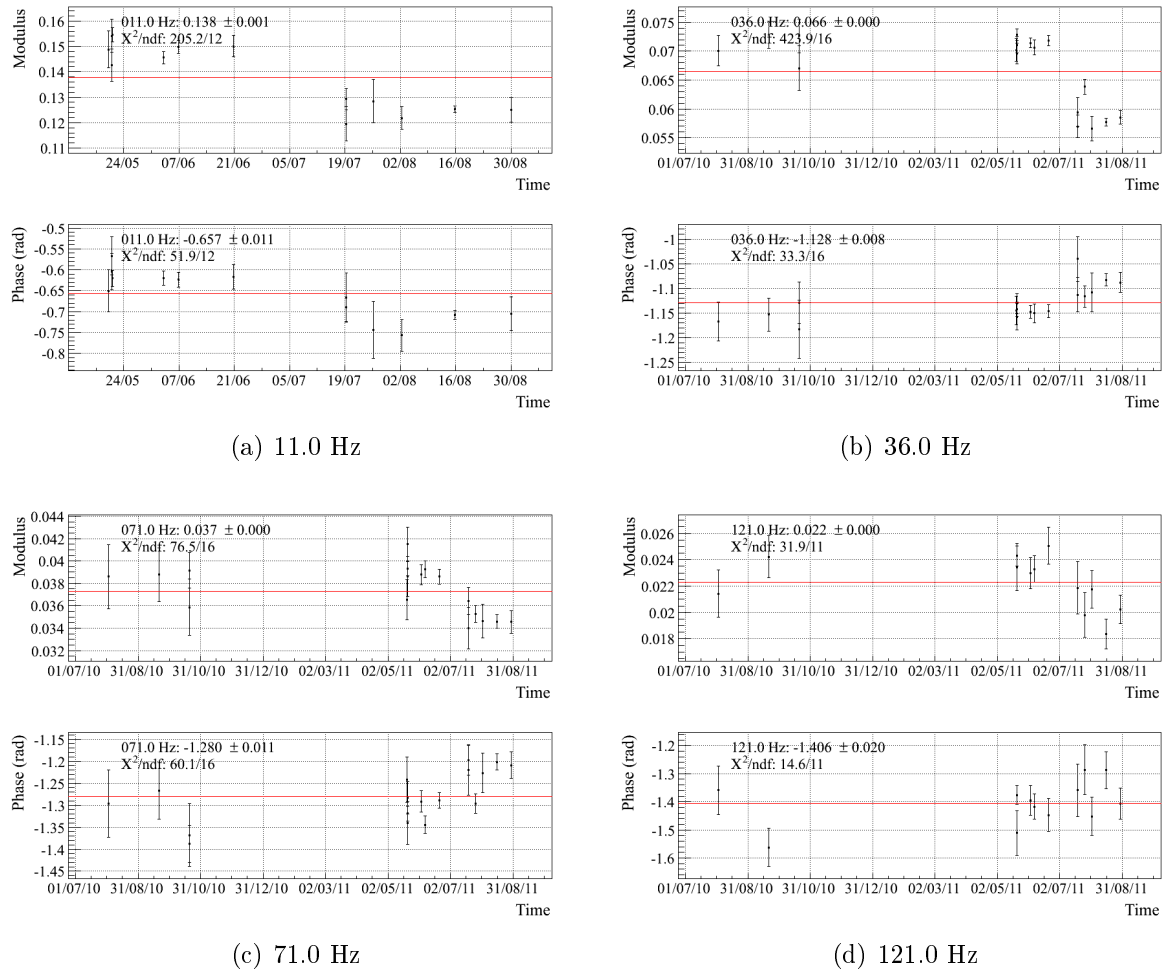


Figure 46: Measured NE marionette to mirror actuation (NE, U-D coils, LN1) TF ratio as function of time at four different frequencies. The mirror and marionette actuations have been corrected for their pendulum mechanical models.